# Treatment of Anaerobic Digestate Using Microfiltration and Ultrafiltration for Pretreatment and Nanofiltration and Reverse Osmosis for Polishing

DEPARTMENT OF PROCESS AND LIFE SCIENCE ENGINEERING | LUND UNIVERSITY
GONÇALO MACHATINE | THESIS 2026

# Treatment of Anaerobic Digestate Using Microfiltration and Ultrafiltration for Pretreatment and Nanofiltration and Reverse Osmosis for Polishing

by

Gonçalo Simão Machatine

Division of Chemical Engineering
Department of Process and Life Science Engineering
Lund University

June 2026

Supervisor: **Mikael Sjölin**
Examiner: **Frank Lipnizki**

Picture on front page: Jeppo Biogas, AB. Photo by Gonçalo Machatine

| **Postal address** | **Visiting address** | **Telephone** |
|---|---|---|
| Box 124 | Kemicentrum | +46 46-222 82 85 |
| SE-221 00 Lund, Sweden | Naturvetarvägen 22 | +46 46-222 00 00 |
| **Web address** | 223 62 Lund, Sweden | |
| http://www.ple.lth.se | | |

Membrane Engineering for Sustainable Development

Funded by the European Union

# Treatment of Anaerobic Digestate Using Microfiltration and Ultrafiltration for Pretreatment and Nanofiltration and Reverse Osmosis for Polishing

Master in Membrane Engineering for Sustainable, MESD

Erasmus Mundus Joint Master

Gonçalo Simão Machatine

June 2026

Lund University

Supervisor: **Mikael Sjölin**

Examiner: **Frank Lipnizki**

Membrane Engineering for Sustainable Development

Funded by the European Union

This master thesis project has been conducted as part of the Erasmus Mundus Joint Master Degree in *Master in Membrane Engineering for Sustainable Development, MESD*, funded by the European Union.

The author thanks the European Commission - Education, Audiovisual and Culture Executive Agency (EACEA) for the Erasmus Mundus scholarship under the program: Master in Membrane Engineering for Sustainable Development, MESD, Project number: 101081874, Call: ERASMUS-EDU-2022-PEX-EMJM-MOB



Université de Montpellier · Université de Toulouse · University of Chemistry and Technology Prague · Lund University · KU Leuven · Universidad Zaragoza · NOVA School of Science & Technology · University of Twente. · Istituto per la Tecnologia delle Membrane Consiglio Nazionale delle Ricerche · Università della Calabria

# Preface

I am grateful to all my family members, friends, and classmates with whom I studied, as well as all the people I met who made these two years so special.

I want to thank my supervisor, Mikael Sjölin, for his support, guidance, and the knowledge he shared throughout this journey.

I sincerely thank Henri Malmi and Riina Kujala at Jeppo Biogas for the opportunity to work on this topic and to develop this project in collaboration with the company.

I would also like to express my gratitude to everyone who, directly or indirectly, contributed to my studies and to the completion of this work.

I would also like to acknowledge that this thesis has in part been produced with the assistance of generative AI tools. Grammarly AI and ChatGPT were used for language correction, grammar checking, and readability improvements. AI-assisted tools were also used to support the development of some MATLAB code for plotting figures, and I reviewed, modified, and validated the code and all resulting figures myself. I take full responsibility for all content, analyses, figures, and conclusions presented in the thesis.

# Popular Scientific Summary

Anaerobic digestion is a common method used to produce biogas from organic waste, but it also generates a leftover material called digestate. Although digestate contains useful nutrients such as nitrogen, phosphorus, and potassium, it can also cause environmental problems such as water pollution, nutrient runoff into rivers and lakes, and unpleasant odors if not properly treated.

One possible treatment method is membrane filtration, which is a process where water is passed through very fine filters (membranes) that allow water molecules to pass through while retaining particles, contaminants, and dissolved substances depending on the membrane type. However, the high amount of solids in digestate can block the membranes and reduce their efficiency over time.

In this study, different membrane filters were tested to clean digestate. The treatment was done in several stages, and each stage removed smaller and smaller contaminants from the water. First, a screen removed large pieces of material such as straw, fibers, and other solid particles that were floating in the liquid. Then the liquid passed through an ultrafiltration membrane, which removed smaller particles such as fine suspended solids, bacteria, and small organic particles. After that, nanofiltration was used to remove even smaller unwanted substances. Finally, reverse osmosis was used, which is the strongest cleaning step and removes almost everything from the water, including dissolved salts, nutrients, and very small contaminants, allowing mainly water molecules to pass through. Each step made the liquid cleaner by removing smaller and smaller particles, resulting in much cleaner water at the end.

The study showed that when higher pressure was used, more water could pass through the filters, but the filters also became clogged faster. Microfiltration membranes clogged more easily than ultrafiltration membranes because their larger pores allowed more particles to get stuck inside. Ultrafiltration was good at removing particles and phosphorus from the water. However, nutrients like nitrogen and potassium were harder to remove because they were dissolved in the water. Nanofiltration removed only a small amount of these dissolved substances. Reverse osmosis worked best and removed most of the remaining pollution, especially phosphorus and organic material. However, nitrogen levels in the final treated water were still higher than the discharge limits, indicating the need for additional treatments to meet environmental requirements.

# Summary

Many studies on anaerobic digestion mainly focus on biogas production, while fewer studies focus on the management of the residual material left after the anaerobic digestion which is digestate. Digestate treatment is important to promote nutrient recovery and support circular economy. Membrane filtration can be used for digestate treatment however, the high solids content of digestate causes severe membrane fouling, reducing membrane performance. Therefore, this study aimed to investigate pre-treatment methods before membrane filtration in order to reduce membrane fouling during ultrafiltration and subsequent polishing using nanofiltration and reverse osmosis membranes.

Screening and coagulation were investigated as pre-treatment methods, although only the screened digestate was used during the membrane filtration experiments. For ultrafiltration (UF), two membranes with pore sizes of 0.04 µm and 1.2 µm were tested. The 0.04 µm membrane was operated at transmembrane pressures of 1, 1.5, and 2 bar, while the 1.2 µm membrane was operated at 1 and 2 bar. The Vibro-Lab system (Sani Membranes), in order to investigate whether vibration-assisted filtration could help reduce membrane fouling and improve filtration performance.

The filtered digestate obtained from UF was then used as feed for nanofiltration (NF) and reverse osmosis (RO). NF and RO experiments were carried out using a DuPont FilmTec NF270 membrane and an Alfa Laval RO99 membrane, respectively. The filtration experiments were conducted using a laboratory-scale dead-end filtration cell. NF experiments were performed at pressures of 5, 10, and 15 bar, while RO experiments were conducted at 15 and 18 bar.

The results showed that increasing transmembrane pressure increased permeate flux but also increased membrane fouling and reduced membrane permeability. UF achieved high rejection of phosphorus and dry matter, while nitrogen and potassium rejection remained lower. NF showed low rejection of nitrogen and phosphorus. In contrast, RO achieved higher rejection of COD and phosphorus, although nitrogen rejection remained lower. Despite the improved permeate quality obtained with RO, the final permeate concentration still exceeded the targeted discharge standards, indicating that additional post-treatment or additional RO stages would likely be required, especially for nitrogen removal.

# Table of Contents

# 1. Introduction

## 1.1. Background

The energy demand has been increasing over the years, requiring greater energy production to meet this demand. Due to current environmental problems such as climate change, global warming, and the emission of other toxic compounds resulting from the use of fossil fuels, there is a need to shift towards cleaner and more sustainable energy sources, in this case, renewable energy sources such as solar, wind, hydro, and biomass.

Biomass is a very attractive option because it uses organic resources such as waste to produce energy. This promotes the circular economy and the minimization of waste generation while simultaneously reducing pollution and generating energy (Hidalgo et al., 2026).

Biogas is a renewable energy source derived from biomass. Biomass used for energy production can be classified into two main categories: dedicated energy crops, which are cultivated specifically for energy purposes, and organic residues and wastes. Examples of wastes include food waste, manure, industrial waste, slaughterhouse waste, food greases, and other biodegradable materials such as vegetables and fruits. Examples of dedicated energy crops include maize silage, grass, and other grown feedstocks (Gent et al., 2017; Hidalgo et al., 2026).

Biogas is produced through anaerobic digestion (AD). During this process, organic matter is broken down by microorganisms in the absence of oxygen, and the biomass is converted into methane and carbon dioxide. The main components of biogas are methane ($CH_4$, 50–70%), carbon dioxide ($CO_2$, 30–50%), and other trace compounds such as water and hydrogen sulfide ($H_2S$) (Jameel et al., 2024). Biogas has many advantages, including energy production, reduction of waste and pollution from agricultural and industrial activities, and the conversion of waste into fertilizer, which reduces the need for mineral fertilizers. In addition, by generating energy, biogas also contributes to decreasing the use of fossil fuels (Plana and Noche, 2016; Jameel et al., 2024)

However, during anaerobic digestion, a portion of the feedstock is not completely degraded and exits the system as an effluent known as digestate. Digestate consists of both solid and liquid fractions and contains undigested organic matter, inorganic compounds, water, and nutrients (Kaur et al., 2020; Nayak and Ranade, 2025). According to Turley et al. (2016), approximately 80–90% of the initial feedstock is converted into digestate. On average, a biogas plant produces around 20 $m^3$ of digestate annually per kilowatt of installed electrical capacity. Compared to conventional fertilizers, digestate is characterized by having low dry matter and nutrient concentrations as well as a high water content. Consequently, large storage volumes are required either near the biogas production facility or close to the application area (Plana and Noche, 2016).

According to the European Biogas Association (2023), around 31 million tons (Mt) of digestate dry matter were produced in Europe in 2022, and this number is expected to grow to 75 Mt of dry matter per year by 2030 and increase to 177 Mt of dry matter per year by 2050.

After exiting the AD process, digestate is stored and transported to agricultural fields, where it is applied to the soil as fertilizer for crops without the need for any further processing (Drosg et al., 2015). However, there are some potential problems and risks related to the use of digestate.

Zielińska and Mikucka (2021) mention that these problems include contamination of surface and ground water by leaching of nutrients, nutrient run-off, eutrophication, soil contamination, and risk to human health by contaminating food due to the presence of pathogens on digestate. In addition, there are other problems, such as the fact that digestate must be stored at biogas plants until it can be applied to agricultural fields. Additionally, greenhouse gases such as carbon dioxide, methane, and nitrous oxide, as well as atmospheric pollutants including ammonia, may be released during digestate storage and land application (Ülgüdür *et al.*, 2019). The required storage period is influenced by several factors, including environmental restrictions on application, digestate stabilization, geographical location, soil and crop type, and digestate demand.

Storage represents a high cost for the biogas system and requires land, while transportation costs are also critical due to the high-water content of digestate, making logistical efficiency essential for the profitability of both the product and the biogas sector. Limitations on the times of year when digestate can be spread often result in long and costly storage periods, which can reduce its economic value. Additionally, prolonged storage can lead to the emission of gases such as $CH_4$, $CO_2$, $NH_3$, and $N_2O$, nutrient leaching, and heavy metal accumulation, contributing to atmospheric pollution (Kaur et al., 2020; Ahrends et al., 2022).

Most studies on biogas focus on anaerobic digestion efficiency and overlook digestate management. However, finding ways to use digestate effectively is as important as improving biogas production.

To reduce digestate volume, membrane separation technologies such as microfiltration, ultrafiltration, nanofiltration, and reverse osmosis can be used. These allow separation and purification of the water fraction, enabling water reuse or compliance with discharge regulations. However, digestate typically contains high dry matter content, high concentrations of suspended solids, organic matter, and colloidal material, which limit the direct application of membrane filtration due to rapid fouling and flux decline. Therefore, appropriate pretreatment is required to make the digestate feed suitable to be used in membrane filtration.

The motivation for this degree project is to evaluate membrane-based treatment of digestate effluent. The study focuses on membrane performance, including flux, fouling, cleaning requirements, and rejection. Microfiltration and ultrafiltration were applied as initial treatment steps, followed by nanofiltration and reverse osmosis as polishing stages to improve water quality for potential discharge or reuse.

This degree project is structured into five chapters. The first chapter provides an introduction, including the background, motivation, and objectives of the study. This is followed by a literature review presenting the current state of technologies for digestate management. The third chapter describes the methodology, outlining the methods and experimental approach used. The fourth chapter presents and discusses the results, and the final chapter provides the conclusions.

## 1.2. Aim

This study aimed to investigate Microfiltration (MF) and Ultrafiltration (UF) as a pretreatment step for digestate, analyze MF and UF membrane performance in terms of flux, fouling behavior, cleaning needs, and rejection, investigate nanofiltration (NF) and reverse osmosis (RO) as a polishing step, and analyze nutrient and contaminant removal efficiency.

# 2. Literature Review

## 2.1. Biogas digestate

Digestate is the residual material left after the anaerobic digestion (AD) process. During AD, microorganisms break down organic feedstocks (such as manure, food waste, or crop residues) in the absence of oxygen to produce biogas. The portion of the substrate that is not converted into biogas remains as digestate (Drosg et al., 2015).

Digestate volumes are usually up to 90% of that of the feedstock fed into the anaerobic digester, and all the nutrients present in the feedstock, including nitrogen (N), phosphorus (P), and potassium (K), remain in the digestate after digestion. However, they are generally in forms that are more readily available for plant uptake compared to those in the original feed materials (Turley et al., 2016).

## 2.2. Characteristics of digestate

Digestate exhibits diverse physicochemical and biological characteristics, which are influenced by the type and composition of the substrates used, as well as operational parameters such as pH, temperature, hydraulic retention time, organic loading rate, and microbial diversity. Studies indicate that digestate generally has a lower total solids (TS) content compared to the original substrate. However, this reduction depends on the initial TS content of the feedstock. Typically, wet anaerobic digestion operates with substrates containing 3–15% TS, whereas dry anaerobic digestion can accommodate substrates with total solids content of up to 30% (Issah et al., 2020).

According to Nayak and Ranade (2025), the variation in digestate composition and nutrient availability makes its use challenging and may limit the growth of biogas industries. During anaerobic digestion, simple organic matter is easily converted into methane ($CH_4$) and carbon dioxide ($CO_2$), while complex compounds like lignin remain, increasing the digestate's organic carbon content. Digestate also contains suspended and colloidal organics, complex nitrogen and phosphorus, and substantial amounts of macronutrients (N, P, K, S, Mg, Ca) and micronutrients (B, Cl, Cu, Fe, Mn, Mo, Ni, Zn).

The **Table 2.1** shows the main properties of different whole digestates from various feedstocks.

*Table 2.1: Physicochemical and nutrient characteristics of whole anaerobic digestates. Values represent typical ranges for digestates derived from various substrates, including food waste, agricultural residues, manure, sludge, and compost. Data were compiled and adapted from Selvaraj et al. (2022), which summarizes multiple studies.*

| Parameter | Typical Feedstock Examples | Range |
|---|---|---|
| **pH** | Food waste, agricultural residues, manure, sludge, compost | 7.1 – 8.9 |
| **Total Solids (TS, %)** | Food waste, manure, agricultural residues, compost | 1.4 – 34.2[1] |
| **Volatile Solids (VS, % of TS)** | Food waste, manure, sludge, compost | 12.3 – 81.5[1] |
| **Total Carbon (TC, g/kg DM)** | Food waste, agricultural residues | 300 – 452[1] |
| **Total Nitrogen (TN, kg/m³)** | Food waste, manure, sludge | 3.5 – 157[1] |
| **Ammonium Nitrogen ($NH_4^+$-N, kg/m³)** | Food, manure, sludge | 1.5 – 108[1] |
| **Total Phosphorus (TP, kg/m³)** | Food waste, manure, sludge | 0.06 – 66[1] |
| **Total Potassium (TK, kg/m³)** | Food waste, manure, agricultural residues | 0.02 – 100[1] |
| **Sulphur (S, g/kg)** | Food waste | 6 – 10[1] |
| **Calcium (Ca, g/kg)** | Food waste | 3 – 10[1] |
| **Magnesium (Mg, g/kg)** | Food waste, agricultural residues | 10 – 52[1] |

[1] Ranges reflect combined values for digestates from multiple substrates

## 2.3. Pre-treatment methods for digestate wastewater

The first step in digestate processing is usually mechanical separation into liquid and solid fractions, using equipment such as centrifuges, decanter screw presses, or sieve belt/drum presses. The use of coagulants or flocculants can improve separation efficiency. Nutrients are unevenly distributed between the fractions: phosphates mainly remain in the solid fraction, while nitrogen and potassium are mostly in the liquid fraction (see

**Table** 2.2). The solid fraction is often dried or composted to make it easier to handle and use (European Biogas Association, 2024).

*Table 2.2: Digestate separation into solid and liquid and nutrient distribution across the two phases. Table adapted from: Exploring digestate's contribution to healthy soils, European Biogas Association. March 2024.*

| Component | Liquid Phase (%) | Solid Phase (%) |
|---|---|---|
| **Nitrogen – Ammonium ($N–NH_4^+$)** | 95 | 5 |
| **Nitrogen – Organic (N–Organic)** | 5 | 95 |
| **Potassium (K)** | 80 | 20 |
| **Phosphorus (P)** | 50 –1 | 50 – 99 |
| **Fibrous Material**[2] | 0 | 100 |
| **Volume** | 80 –90 | 10 – 20 |

### 2.3.1. Liquid/Solid Separation

Solid–liquid separation is usually the first step before further processing. The objective is to mechanically separate the digestate into a liquid and solid fraction. This can reduce the volume requiring storage by approximately 10–20% of the original digestate volume. (European Biogas Association, 2024).

#### *2.3.1.1 Screw Press*

The screw press is the most commonly used equipment for digestate separation. It separates solids and liquids based on particle size by forcing digestate against a mesh screen. Liquids and particles smaller than the mesh pass through, forming the liquid fraction, while larger solids are pressed toward an outlet flap (see **Figure 2.1**). Digestate is pushed into a rotating screw inside a screening

[2] Depend on the use of coagulants / flocculants for solid phase separation

drum with small holes, with an opening between 0.5 –1 mm (Cathcart et al., 2023; Fechter and Kraume, 2016)

By adjusting the pressure, screen size, and flap resistance, the dryness of the solid fraction can be controlled. Smaller screens retain finer particles in the solids, while larger screens allow some fine particles to pass into the liquid, lowering solids separation efficiency. The result is solids that are easier to handle and a nutrient-rich liquid that can be reused or applied as fertilizer (Cathcart et al., 2023; European Biogas Association, 2024).

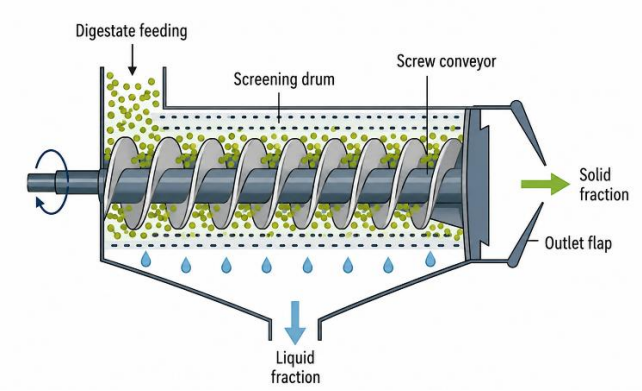


*Figure 2.1: Schematic representation of a screw press. Adapted from: Fachverband Biogas e.V., 2018.*

#### *2.3.1.2 Decanter Centrifuge*

The decanter centrifuge is another common machine used for digestate separation. Unlike the screw press, which separates based on particle size, the decanter centrifuge separates based on density (Fechter and Kraume, 2016).

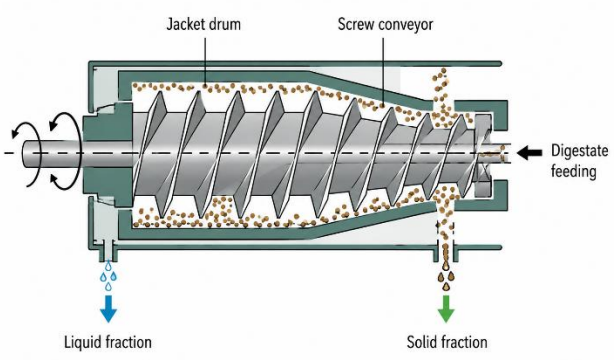


*Figure 2.2: Schematic representation of a decanter. Adapted from: Fachverband Biogas e.V., 2018.*

In this system **(Figure 2.2**), digestate is spun in a rapidly rotating bowl, where denser solid particles are forced outward against the bowl wall due to centrifugal force. A screw conveyor, rotating at a slightly different speed than the bowl, transports the accumulated solids to a solids discharge port.

The liquid fraction exits through the space between the screw conveyor and the drum. Decanter centrifuges can recover smaller particles than a screw press, which is limited by the mesh screen size (Cathcart et al., 2023).

The degree of separation can be adjusted by changing the rotational speeds of the bowl and screw, as well as the throughput. As a result, decanter centrifuges typically achieve a very high level of separation, producing drier solids and clearer liquid compared to screw presses (European Biogas Association, 2024).

The decanter centrifuge is especially suitable for applications where phosphorus recovery is the main objective, while the screw press may be preferable in situations where lower investment and operating costs are the primary concern.

Furthermore, according to Nowak and Czekała (2024), for biogas plants processing agricultural waste and energy crops, the screw press is a more suitable solution than a centrifuge.

In addition to these technologies, screening systems such as vibrating screens or drum screens can be applied either independently or in combination with screw presses or decanter centrifuges. In screening systems, the liquid fraction passes through the screen openings, whereas the solid fraction is retained and conveyed to the discharge outlet. This technique is applied exclusively to remove solids from liquids with a low dry matter content. The typical screen slit width ranges from 150 to 250 μm (Al Seadi *et al*., 2013; European Biogas Association, 2024; Fechter and Kraume, 2016).

### 2.4.1. Liquid Treatment

#### *2.4.1.1. Evaporation*

Evaporation removes water from digestate by heating it, separating it from contaminants such as salts, heavy metals, and organic compounds. The result of this process is a concentrated digestate that has most of its original nutrients, however, significant losses of ammonia can occur during the process. Purified water vapor is also generated, which can be condensed and reused or discharged into receiving water bodies. (Khan et al., 2024). Furthermore, evaporation reduces the volume of digestate, facilitating storage and lowering transportation costs.

The evaporation process begins with pre-treatment, where the liquid digestate is screened to remove large solids. It is then pumped to the evaporation unit and heated to promote water evaporation. In the evaporator, water is vaporized and later condensed for reuse or discharge, while the remaining digestate becomes more concentrated, increasing its solids content. The concentrated digestate is subsequently cooled and stored for further use, typically as fertilizer (Fachverband Biogas e.V., 2018). During the process, gaseous emissions, particularly ammonia and water vapor, are captured and directed to a scrubber, where ammonia reacts with sulfuric acid to form ammonium sulphate. This helps reduce emissions while recovering nitrogen in a usable form (Khan et al., 2024).

#### *2.4.1.2. Coagulation – Flocculation.*

Coagulation–flocculation is a solid-liquid separation process used to enhance the elimination of suspended solids and colloidal particles that cause turbidity (Xavier et al., 2020).

Raw digestate contains high levels of negatively charged colloids and fine particles, which repel each other and hinder sedimentation or flotation. Coagulants, typically multivalent cations, neutralize these charges and promote particle aggregation through flocculation Canadian Biogas Association (2024). A Jar test is generally required to select the coagulant and to determine the appropriate dosage. Common coagulants include aluminum sulfate ($Al_2(SO_4)_3$), ferric chloride ($FeCl_3$), and ferric sulfate ($Fe_2(SO_4)_3$).

However, the use of these chemicals introduces additional ions such as iron or aluminum in the solids, and sulfates or chlorides in the liquid, which should be considered in downstream processing or when evaluating the suitability of the final digestate products (Canadian Biogas Association (2024).

### 2.5. Membrane Technologies used for digestate treatment

Membrane filtration is an efficient and economical method for separating suspended or dissolved substances in a liquid. The membrane serves as a selective barrier, allowing certain molecules to pass based on their size or chemical properties (Calabrò & Basile, 2011). In addition, membranes have certain advantages such as high efficiency during separation, stable permeate quality and reduced chemical consumption (Ren *et al.*, 2026). Common membrane processes used for digestate treatment include microfiltration (MF), ultrafiltration (UF), nanofiltration (NF), and reverse osmosis (RO) (Barampouti et al., 2020).

The retention capability of a membrane is determined by its molecular weight cut-off (MWCO), which corresponds to the membrane's pore size. Membrane pore sizes range from 0.1 nm to 10000 nm, depending on the type. **Table 2.3** presents the classification of the main commercial membrane processes used for the treatment of digestate liquid fractions, together with their typical pore sizes.

*Table 2.3: Classification of commercial membrane filtration processes used for digestate liquid fraction treatment and their typical pore size ranges. Adapted from DuPont Water Solutions (2025) and Camilleri-Rumbau et al., 2021.*

| Process | MF | UF | NF | RO |
|---|---|---|---|---|
| **Pore Size** | 0.1–10 μm | 0.01 to 0.1 μm | 0.001 to 0.01 μm | 0.0001 to 0.001 μm |
| **Material Retained** | Suspended solids and large colloids | Viruses and large proteins | Micropollutants and divalent ions | Dissolved salts |
| **Permeate** | Water and dissolved solutes | Water, salts, and smaller molecules | Water and monovalent salts | Water |
| **Operating Pressure** | 0.1 – 2 bar | 1 – 7 bar | 3.5 – 16 bar | 5 – 84 bar |

After solid/liquid separation, the liquid fraction of digestate can be treated using membrane filtration processes to increase nutrient concentration and improve water recovery. However, membrane fouling is one of the main operational limitations because it decreases membrane performance and reduces long-term continuous operation. Fouling is influenced by multiple factors, including membrane characteristics such as pore size, material, surface morphology, porosity, and ion rejection capacity, as well as operating conditions and the physicochemical properties of the digestate (Camilleri-Rumbau et al., 2021). As a result, membranes often require frequent cleaning and replacement, increasing operational and maintenance costs (Zielińska and Mikucka, 2021; Zhu *et al.*, 2026).

Membrane fouling occurs when particles and other contaminants accumulate on the membrane surface or inside its pores, causing a reduction in filtration efficiency and permeate flux. Fouling can be either reversible or irreversible depending on whether the deposited materials can be removed during cleaning. The main fouling mechanisms include pore blockage, cake layer development, and pore narrowing. To control fouling, different physical and chemical cleaning techniques have been applied, such as flushing, backwashing, and chemical cleaning procedures. These methods can enhance membrane flux recovery by removing deposited foulants and reducing the buildup of fouling layers on the membrane surface (Zhao *et al.*, 2025)

Vibrating membrane modules or Vibratory shear enhanced processing (VSEP) are advanced membrane filtration systems designed to reduce membrane fouling and improve filtration performance. In addition, they are considered particularly suitable for the treatment of highly concentrated streams such as digestate and manure effluents, which contain high concentrations of suspended solids and organic matter.

Vibrating membrane systems reduce membrane fouling by generating shear forces at the membrane surface through oscillatory motion or vibration, unlike conventional membrane systems that primarily depend on crossflow velocity (Jaffrin and Ding, 2015; Vega et al., 2022). The resulting turbulent flow reduces the laminar boundary layer, increases shear stress on the membrane surface, and promotes mixing near the membrane, thereby limiting the deposition of particles and cake layer formation (Zhao et al., 2023).

For digestate processing, MF and UF are commonly used as pretreatment steps before NF and RO in order to reduce membrane fouling and improve overall filtration performance. To further purify the permeate, NF and RO are applied for the removal of dissolved compounds and nutrient concentration. Barampouti et al. (2020) reported separation efficiencies of 5–23% for ammonium nitrogen and 97 – 98% for phosphorus using NF. While in RO systems, recovery efficiencies of 99 – 100% were achieved, producing high-quality permeate with very low pollutant concentrations.

RO membranes are capable of producing high-quality water suitable for reuse or discharge. However, conventional membrane systems frequently encounter operational challenges during digestate treatment, mainly due to membrane fouling and clogging. Vaneeckhaute et al. (2019) reported the application of vibrating shear-enhanced processing technology for digestate treatment. Their study demonstrated successful recovery of nitrogen-, phosphorus-, and potassium-rich mineral concentrates while simultaneously producing water suitable for discharge. Nevertheless, the treated effluent did not consistently meet the Flemish discharge limits for surface waters, which are set at COD 125 $mgL^{-1}$, 15 mg N $L^{-1,}$ and 2 mg P $L^{-1}$.

## 2.6 Description of Jeppo Biogas

Jeppo Biogas AB (Jepuan Biokaasu Oy) is a biogas plant located in Kauhava, Ostrobothnia, Finland. The plant has been in operation since 2013 and was expanded in 2020 to include a separate dry fermentation section in addition to the original wet fermentation section. The plant produces approximately 45 GWh of biogas per year (Jeppo Biogas., 2026).

The annual feedstock input at Jeppo Biogas is approximately 160,000 tons. Pig slurry constitutes the largest fraction (87,000 t/year), followed by slaughterhouse waste (40,500 t/year), fats from various sources (13,790 t/year), potato-related waste (8,400 t/year), and other organic substrates including vegetables, grass, and grains (10,310 t/year).

The Jeppo Biogas plant has three bioreactors, each with a capacity of 4000 $m^3$. Raw materials are supplied to the reactors through a pipeline system that includes storage tanks for digestate. There are six storage tanks located on-site, as shown in **Figure 2.3**.

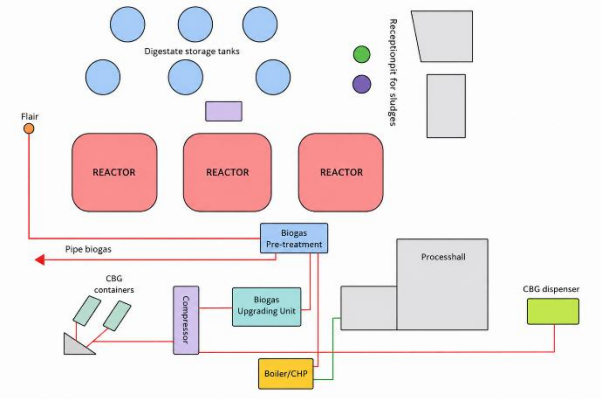


*Figure 2.3: Schematic of Jeppo Biogas Production Process. Adapted from: (Sherman, 2016).*

The fermentation process is wet, allowing continuous feeding of raw materials into the reactors. Before entering the bioreactors, the biomass mixture is pre-treated to reduce particle size, which facilitates digestion by microorganisms (Sherman, 2016).

At Jeppo Biogas, organic raw materials are mixed and digested for 20 – 30 days. After digestion, carbon dioxide is removed from the biogas, increasing the methane content to 98 – 99%, making it suitable for use as vehicle fuel and for heat production in industrial and district heating plants. (Jeppo Biogas., 2026).

# 3. Materials and Methods

## 3.1. Location of Study

Pilot-scale experiments were conducted at the industrial site of Jeppo Biogas AB, located in Kauhava, Finland, over a period of approximately one month. The pretreatment strategies investigated were screening and coagulation–flocculation. These pretreatment approaches were assessed to determine their potential to reduce fouling and improve membrane performance. The second phase of the experimental work, involving nanofiltration (NF) and reverse osmosis (RO) testing of the permeate stream obtained at Jeppo Biogas and it was conducted at the pilot hall laboratory of the Faculty of Engineering at Lund University, Sweden.

## 3.2. Microfiltration and Ultrafiltration Experiments

### 3.2.1. Materials & Equipment

#### *3.2.1.1 Digestate*

The raw digestate was obtained from the digestate storage tank at Jeppo Biogas and stored in a 1 $m^3$ intermediate bulk container (IBC). Before use, the digestate was thoroughly mixed to prevent sedimentation of suspended solids. After homogenization, the digestate was transferred to a 40 L tank, which served as the feed tank during the filtration experiments.

#### *3.2.1.2 Membranes*

Two membrane cartridges were used. The membranes were supplied by Sani Membranes A/S, Denmark:

- **MicroPES™ 1F M** – pore size: **0.04 µm**
- **MicroPES® 12F** – pore size: **1.2 µm**

Both membranes share similar operational specifications. The system operates within a media temperature range of 5 – 55 °C. The operating pressure range is 0 – 3 bar at temperatures between 5 – 35 °C and 0 – 1 bar at temperatures up to 55 °C. The allowable pH range is 1 – 13, and the apparent viscosity range is 1 – 1000 cP. The membrane area of the system is 0.35 $m^2$.

#### *3.2.1.3 Equipment*

- **Stirrer:** Ensured homogeneous mixing of the feed solution.
- **Thermometer:** Used to measure the temperature at the beginning of each experiment. **Electronic Balance:** Used to record permeate mass at regular time intervals.
- **Sieves:** A sieve with an opening size of 1 mm was used for pre-treatment of the digestate.
- **Membrane Filtration System:** Filtration experiments were conducted using a bench-scale membrane system, the VibroLab 35000 from Sani Membranes. The Figure 3.1 shows the setup used for the filtration experiments.

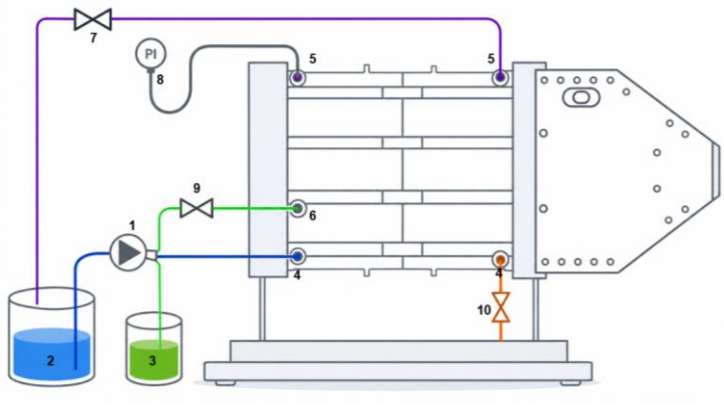


*Figure 3.1: VibroLab system schematic. Adapted from: Sani Membranes user manual Vibro-Lab3500, SANI Membranes A/S.*

The VibroLab 3500 membrane filtration system consisted of a peristaltic feed pump (1), a feed/retentate vessel (2), a permeate collection vessel (3), a retentate valve (7), a pressure gauge (manometer, 0–4 bar) (8), a permeate valve (9), and a drain valve (10). The feed pump circulated the feed solution through the system, while the feed/retentate and permeate vessels were used for sample collection. The retentate, permeate, and drain valves controlled the flow during operation, and the pressure gauge was used to monitor the operating pressure.

### 3.2.2. Procedures

#### *3.2.2.1 Membrane Conditioning*

Before starting the filtration experiments, the membranes were conditioned by chemical cleaning. A 10 L cleaning solution containing 0.8% sodium hydroxide (NaOH) at 55 °C. was prepared. This solution was circulated through the membrane module for 20 minutes to ensure full contact with the membrane surface. Following the chemical cleaning, a hot water flush at 55 °C was performed to remove any residual cleaning solution.

All water used for cleaning, flushing, and pure water flux measurements was prepared using potable water, as it was the best available water source on site.

#### *3.2.2.2 Pure Water flux measurements*

After membrane conditioning, the initial water flux was determined using potable water as the feed. The operating conditions, including temperature and transmembrane pressure (TMP), were set according to the experimental plan. Filtration was continued until the feed tank was emptied, while permeate mass was recorded over time.

After subsequent cleaning, a second water flux was measured under the same conditions. The difference between the initial water flux and the second water flux was used to evaluate fouling, representing foulants that could not be removed by chemical cleaning.

#### *3.2.2.3 Digestate Flux Measurements*

Digestate filtration experiments followed the same procedure as the pure water flux measurements, with digestate used as the feed solution. Due to the higher viscosity and solids content of the digestate, filtration was significantly slower. Therefore, experiments were conducted over fixed durations of 1 hour. During filtration, permeate mass and time were continuously recorded.

#### *3.2.2.4 Membrane Cleaning*

After filtering the digestate in each experiment, the membrane was cleaned using the following procedure:

- Hot water flush (55 °C): Performed to remove loosely attached foulants
- Chemical cleaning: A 0.8% NaOH solution at 55 °C was circulated through the system for 20 minutes.
- Final water flush: Conducted to remove residual cleaning solution.

#### *3.2.2.5 Coagulation*

Coagulation experiments were conducted using:

- **Ferric chloride ($FeCl_3$)**
- **HTH 25**, an organic cationic polymer

Different dosages ranging from 1 to 10 $mL \cdot L^{-1}$ for the HTH 25 and 5 to 20 $mL \cdot L^{-1}$ for the ferric chloride. Due to some limitations, pH adjustment was not possible because neither a pH meter nor pH strips were available on site during the testing period. Additionally, the plant operates under an eco-label certification, which limited the use of chemical additives in the process. As a result, coagulation experiments were performed on a limited scale.

Two types of feed were used:

- Sieved digestate (1 mm)
- Raw (unsieved) digestate

The primary variable investigated was the type of coagulant ($FeCl_3$ vs. HTH 25), rather than dosage optimization or pH control. The objective of the coagulation tests was to determine whether coagulation or floc formation would occur when the digestate was treated with coagulants, rather than to optimize the process.

### 3.2.3. Experimental Design

Two membrane pore sizes were evaluated to investigate the effect of membrane characteristics and transmembrane pressure on digestate filtration performance. The 0.04 µm membrane was tested at pressures of 1, 1.5, and 2 bar, while the 1.2 µm membrane was operated at 1 and 2 bar. Temperature control was not applied during the experiments because no heating system was available. Therefore, only the initial digestate temperature was measured at the beginning of each filtration experiment.

## 3.3. Nanofiltration and Reverse Osmosis Polishing

The second part of the experiment consisted of polishing the digestate by using nanofiltration and reverse osmosis. To carry out this experiment, the following materials, chemicals, and equipment were used:

### 3.4. Materials & Equipment

#### *3.3.1.1 Digestate - Feed Material*

The filtered digestate used for ultrafiltration (UF) was then collected and sent to the LU pilot hall. The collected samples where it was stored in cold storage until further use.

#### *3.3.1.2 Membranes*

NF and RO experiments were carried out using a DuPont FilmTec NF270 membrane and an Alfa Laval RO99 membrane. The NF270 membrane is a polypiperazine thin-film composite membrane with a maximum operating temperature of 45 °C, maximum operating pressure of 41 bar, and pH operating range of 3 – 10 (DuPont, 2024).

The RO99 membrane is a polyester thin-film composite membrane with a media temperature limit of 50 °C, operating pressure range of 15 – 35 bar, and pH operating range of 3 – 10 (Alfa Laval, 2023).

#### *3.3.1.3 Equipment*

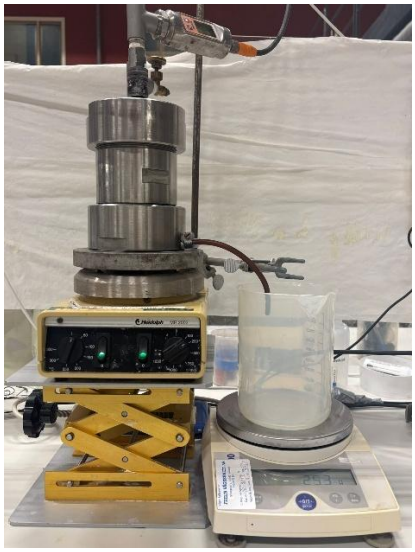

*Figure 3.2: Schematic of the experimental setup for dead-end cell.*

The filtration experiments were conducted using a laboratory-scale dead-end cell. The main instruments used were:

- **Magnetic Stirrer:** Stirring was applied to ensure proper mixing of the feed solution and to reduce the accumulation of solutes near the membrane surface, thereby minimizing concentration polarization.
- **Thermometer:** Used to monitor and maintain the operating temperature throughout the experiment.
- **Electronic Balance:** The permeate mass was recorded at regular time intervals for the calculation of permeate flux.

### 3.4.1. Procedures

#### *3.3.2.1 Membrane Conditioning*

Before starting the experiments, the membrane was chemically cleaned using an alkaline cleaning solution, Ultrasil™ 110 Alkaline Cleaner supplied by Ecolab, prepared at a 100:1 ratio. The solution was filtered through the dead-end stirred-cell module to ensure full contact with the membrane surface.

#### *3.3.2.2 Pure Water Flux Measurement*

After membrane cleaning, the initial pure water flux ($PWF_{Initial}$) was determined using deionized water as the feed solution. The operating conditions, including stirring speed (rpm) and transmembrane pressure (TMP), were adjusted according to the experimental plan. Filtration was continued until all water in the cell had permeated through the membrane.

#### *3.3.2.3 Digestate Flux Measurements*

Digestate filtration experiments followed the same procedure as the initial pure water flux measurements, with digestate used as the feed solution. During filtration, permeate mass and filtration time were continuously recorded.

#### *3.3.2.4 Pure Water Fluxes After Treatment*

After completing digestate filtration, the filtration cell was emptied and gently rinsed with demineralized water. A second pure water flux measurement ($PWF_{Fouling}$) was then conducted under the same operating conditions used for the initial pure water flux test. The comparison between $PWF_{Initial}$ and $PWF_{Fouling}$ was used to estimate reversible fouling, corresponding to the portion of flux decline recoverable without chemical cleaning.

#### *3.3.2.5 Membrane Cleaning*

Following the post-water flux measurement, the membrane was chemically cleaned using the same alkaline cleaning solution described previously for the membrane conditioning. After cleaning, a third pure water flux measurement ($PWF_{Cleaning}$) was performed. The remaining difference between $PWF_{Initial}$ and $PWF_{Cleaning}$ was considered to represent irreversible fouling caused by foulants that could not be removed during chemical cleaning.

### 3.4.2. Experimental Design

The NF and RO experiments were performed under different operating pressures while maintaining constant stirring speed and ambient temperature conditions. The operating temperature corresponded to the ambient temperature of approximately 25 °C. A stirring speed of 250 rpm was applied throughout all experiments. Nanofiltration experiments were conducted at transmembrane pressures of 5, 10, and 15 bar, whereas reverse osmosis experiments were performed at 15 and 18 bar.

### 3.4.3. Calculations

#### *3.3.4.1 Flux*

During the experiment, the permeate mass was recorded every minute, and the flux was calculated using:

$$J = \frac{Q}{A \cdot t} \quad (1)$$

where:

- $J$= flux ($L \cdot m^{-2} \cdot h^{-1}$)
- $Q$= permeate volume (L)
- $A$= membrane active area ($3.2170 \times 10^{-3}$ $m^2$)
- $t$= filtration time (min)

#### *3.3.4.2 Fouling factor*

The fouling factor (FF) was used to quantify the loss in membrane performance due to fouling:

$$FF = \left(1 - \frac{PWF_{Fouling}}{PWF_{Initial}}\right) \times 100\% \quad (2)$$

where:

- $PWF_{Initial}$= initial pure water flux
- $PWF_{Fouling}$= pure water flux after fouling

#### *3.3.4.3 Membrane Rejection*

The membrane rejection (R) was used to evaluate the removal efficiency of the membrane for a specific compound:

$$R = \left(1 - \frac{C_p}{C_f}\right) \times 100\% \quad (3)$$

where:

- $C_f$= feed concentration
- $C_p$= permeate concentration
- $R$= membrane rejection (%)

#### *3.3.4.4 Flux Recovery*

The flux recovery rate (FRR) was used to evaluate the membrane cleaning efficiency:

$$FRR = \frac{PWF_{cleaning}}{PWF_{Initial}} \times 100\% \quad (4)$$

where:

- $PWF_{cleaning}$= pure water flux after cleaning

# 4. Results and Discussion

## 4.1. Screening

The feed was screened using a sieve with an opening size of **1 mm**, as smaller mesh sizes were not available on site. This screening step was implemented to remove large suspended solids and reduce the fouling potential before membrane filtration. By comparing selected parameters in the raw feed and screened feed, we can evaluate the impact of the screening step. The results are shown in **Table 4.1**.

*Table 4.1: Difference between screening and raw feed.*

| Parameter | Raw Feed | Screened Feed |
|---|---|---|
| **Total Nitrogen (N) ($mg \cdot L^{-1}$)** | 4900 | 4343 |
| **Soluble Nitrogen (N) ($mg \cdot L^{-1}$)** | 3200 | 2929 |
| **Soluble Phosphorus (P) ($mg \cdot L^{-1}$)** | 101 | 101 |
| **Dry Matter (%)** | 3.0 | 2.7 |

The screening results showed a smaller reduction in dry matter content from 3.0% to 2.7%, indicating that approximately 10% of the solids were removed during screening, while about 90% remained in the feed. A smaller decrease was also observed for total nitrogen (from 4900 to 4300 mg $L^{-1}$) and soluble nitrogen (from 3200 to 2900 mg $L^{-1}$), suggesting that part of these components was associated with the removed solids. No significant changes were observed for soluble phosphorus, confirming that dissolved compounds are not affected by mechanical screening. It would have been better to use a screen with a smaller opening than those available on site. As this would likely have resulted in a larger reduction of solids or dry matter, which would have further improved the filtration process. With the screens that were used, approximately 90% of the solid material still passed through the screen.

## 4.2. Coagulation

For the biopolymer HTH, very poor or no coagulation was observed in both raw and sieved digestate. Different dosages ranging from 1 to 10 $mL \cdot L^{-1}$ were tested, but no clear floc formation or settling was observed. Based on visual inspection, it was not possible to identify any significant improvement in solid-liquid separation.

Ferric chloride showed better performance than the biopolymer. In the raw digestate, the reaction was weak, although some foam formation was observed during addition, suggesting that a reaction occurred. However, settling remained poor.

In the sieved digestate, $FeCl_3$ showed a more noticeable effect. From right to left (5, 10, and 15 $mL \cdot L^{-1} FeCl_3$), the samples showed improved settling and phase separation. At 5 $mL \cdot L^{-1}$, only a

small reaction was observed. At 10 $mL \cdot L^{-1}$, some floc formation and partial settling occurred, with the appearance of different phases. The best visual result was obtained at 15 $mL \cdot L^{-1}$, where clearer phase separation was observed, and the upper liquid phase appeared less turbid. Increasing the $FeCl_3$ dosage further to 20 $mL \cdot L^{-1}$ did not result in additional improvement. This suggests that screening improved the effectiveness of coagulation by removing part of the coarse solids, although a relatively high $FeCl_3$ dosage was still required to obtain visible coagulation. Due to the high solids content, it is likely that additional solids reduction prior to coagulation would have decreased the coagulant dosage.


*Figure 3: Results of the coagulation tests performed on the sieved digestate samples using $FeCl_3$.*

## 4.3. Microfiltration (MF) and Ultrafiltration (UF)

### 4.3.1. Microfiltration: 1.2 µm Pore Size

**Figure 4.4** presents the flux performance of the 1.2 µm membrane under two different conditions or transmembrane pressures, 1 and 2 bar. The filtration was carried out at 17.4 °C for potable water and 19.5 °C for digestate. The initial water flux was 335.6 ± 20.2 $L \cdot m^{-2} \cdot h^{-1}$ at 1 bar and increased to 379.9 ± 40.5 $L \cdot m^{-2} \cdot h^{-1}$ at 2 bar. This increase is expected, since a higher operating pressure generally provides a greater driving force for permeation across the membrane.

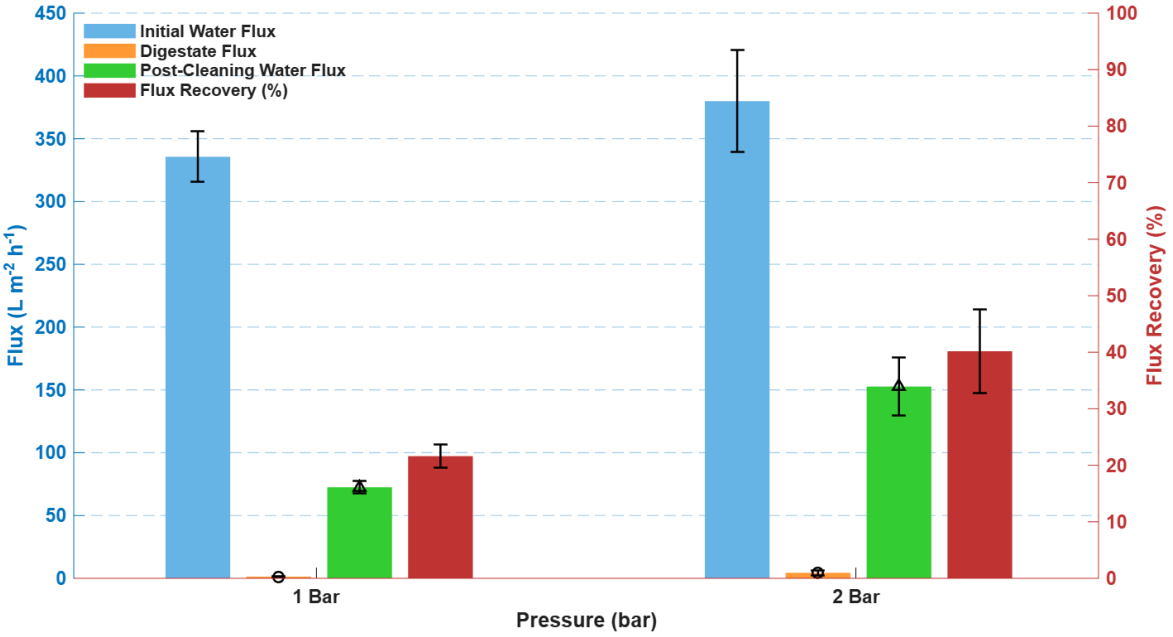


*Figure 4.4: Comparison of pure water flux (PWF), digestate flux, water flux after chemical cleaning, and flux recovery of the 1.2 µm membrane at 1 and 2 bar. Flux values are represented on the left y-axis, while flux recovery (%) is shown on the right y-axis.*

For the digestate, the flux was much lower than the initial water flux, with values of only 1.29 ± 0.45 $L \cdot m^{-2} \cdot h^{-1}$ at 1 bar and 4.33 ± 2.10 $L \cdot m^{-2} \cdot h^{-1}$ at 2 bar. This decline indicates severe fouling during digestate filtration. Camilleri-Rumbau et al. (2021) reported that permeate flux decline typically occurs in two stages: an initial rapid decrease caused by fast fouling formation, followed by a slower and relatively stable filtration period. In this study, this strong flux reduction can likely be caused by the high suspended solids concentration and organic matter content of the digestate, which may have promoted pore blocking and cake layer formation on the membrane surface. This behavior was also observed in ultrafiltration studies by Chuda and Ziemiński. (2023), where digestate filtration showed an initial rapid fouling layer forming on the membrane, followed by the gradual penetration of fine solids, suspended matter, and organic colloids from the liquid fraction of the digestate into the membrane pores.

Although the digestate flux increased at 2 bar, it remained extremely low compared with the water flux, showing that increasing pressure alone was not sufficient to overcome fouling resistance.

After chemical cleaning, the water flux recovery remained limited. The post-cleaning water flux was 72.53 ± 5.13 $L \cdot m^{-2} \cdot h^{-1}$ at 1 bar and 152.63 ± 23.00 $L \cdot m^{-2} \cdot h^{-1}$ at 2 bar. Compared with the initial water flux, this corresponds to a recovery of 21.6 ± 1.9 % at 1 bar and 40.2 ± 7.0 % at 2 bar. The incomplete recovery suggests that a large proportion of the fouling could not be removed by the applied cleaning procedure, indicating that the foulants were strongly attached to the membrane surface or trapped within the membrane pores and therefore could not be fully removed by chemical cleaning.

### 4.3.2. Ultrafiltration: 0.04 µm Pore Size

The **Figure 4.5** shows the flux obtained under different operating conditions in an ultrafiltration process carried out at pressures of 1, 1.5, and 2 bar using a membrane with a pore size of 0.04 µm.

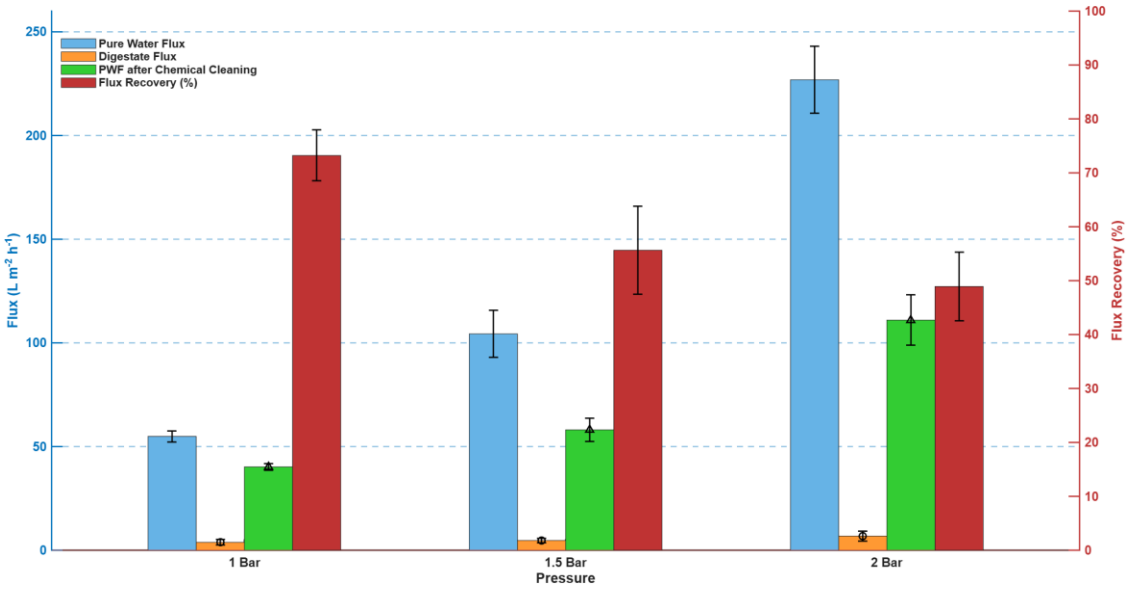


*Figure 4.5: Comparison of pure water flux (PWF), digestate flux, water flux after chemical cleaning, and flux recovery of the 0.04 µm membrane at 1, 1.5, and 2 bar. Flux values are represented on the left y-axis, while flux recovery (%) is shown on the right y-axis.*

From the bar chart, we can see that the water flux increased with increasing transmembrane pressure from 54.9 ± 2.66 $L \cdot m^{-2} \cdot h^{-1}$ at 1 bar to 104.3 ±11.2 $L \cdot m^{-2} \cdot h^{-1}$ at 1.5 bar and 226.9 ± 16.2 $L \cdot m^{-2} \cdot h^{-1}$ at 2 bar.

Although the same pressure-dependent trend was observed for the 1.2 µm membrane, when compared to this membrane, the 0.04 µm membrane had lower pure water fluxes across all pressures. This difference is due to the smaller pore size of the 0.04 µm membrane, which results in higher hydraulic resistance.

As for the digestate flux, both membranes experienced a significant decline in flux, however, the 0.04 µm membrane kept higher digestate flux values compared to the 1.2 µm membrane, with 3.8 ±1.38 $L \cdot m^{-2} \cdot h^{-1}$ at 1 bar, 4.70 ± 1.00 $L \cdot m^{-2} \cdot h^{-1}$ at 1.5 bar, and 6.83 ± 2.43 $L \cdot m^{-2} \cdot h^{-1}$ at 2 bar.

Although the flux increased slightly with pressure, the overall values remained low for both membranes. This indicates that the membrane was strongly affected by fouling during the filtration process. As for the 1.2 membrane, the digestate flux was even lower, especially at 1 bar, suggesting that larger pores of the 1.2 µm membrane allowed more particles to penetrate into the pores, leading to internal pore blocking. Similar observations were reported by Camilleri-Rumbau et al. (2021), who noted that membranes with higher porosity are more susceptible to fouling because increased flow through the membrane can transport more foulants into the pores. Waeger et al. (2010) also reported in their study that the membrane with the largest pore size did not exhibit the highest flux, and they concluded that membranes with larger pores are more susceptible to internal

pore clogging by smaller particles, and membranes with smaller pores are less susceptible to fouling and have higher flux rates.

On the other hand, the 0.04 µm membrane likely retained most foulants on the surface rather than inside the pores, resulting in the formation of a cake layer, which, according to Mustika et al. (2025), also acts as an additional resistance for permeation and results in a decreasing permeate flux.

The water flux after cleaning also shows these differences between the two membranes. The 1.2 µm membrane exhibited low flux recovery of 22% and 40% at 1 and 2 bar, respectively, indicating more irreversible fouling. In contrast, the 0.04 µm membrane showed higher recovery values of 73.2 ± 4.75% at 1 bar, 55.7 ± 8.19% at 1.5 bar, and 48.9 ± 6.4% at 2 bar. Although the 0.04 µm membrane demonstrated better recovery at all pressures, a clear decreasing trend was observed with increasing pressure. This suggests that fouling becomes more severe at higher operating pressures, likely due to increased deposition of particles and compression of the fouling layer.

As reported in fouling studies by Jiang et al. (2018) and Mustika et al. (2025), an increase in pressure generally increases permeate flux; however, it also increases the concentration polarization or accumulation of particles near the membrane surface, creating a localized concentration gradient which promotes the deposition of contaminants and scaling agents, accelerating fouling.

The severe fouling observed during the UF experiments may also be related to the relatively high solids concentration of the screened digestate used in this study. Fechter and Kraume (2016) reported that UF systems can typically cope with concentrations up to 25 g/L, corresponding to a dry matter content of around 2.5%. In the present study, the screened digestate had a dry matter content of approximately 2.7%, exceeding this value. This higher solids concentration may have contributed to accelerated cake layer formation, pore blockage, and the significant flux decline observed during filtration. Waeger et al. (2010) also reported that cross-flow filtration of anaerobic digestate is mainly dominated by cake layer formation due to the high concentration of suspended particles present in the feed.

Additionally, the effect of pressure differed between the two membranes. While increasing pressure improved the initial flux for both membranes, it also led to increased fouling. This effect was more evident for the 0.04 µm membrane, where flux recovery decreased with increasing pressure. At pressures above 2 bar, a strong drop in permeate flux was observed, and permeate flow was temporarily lost. Pressure had to be reduced to restore permeate flow. This suggests that the membrane became more fouled and that flow resistance increased significantly, likely due to pore blockage or strong cake layer formation.

### 4.3.3. Nutrient Rejection after Ultrafiltration

Due to the poor filtration performance observed with the 1.2 µm membrane, the 0.04 µm membrane was selected for further sampling and analysis of additional parameters requested by the company. The membrane rejection values are shown in Table 4.2.

*Table 4.2: Concentrations of some parameters in the screened feed, retentate, and permeate streams after ultrafiltration using the 0.04 µm membrane, together with the calculated membrane rejection values.*

| Parameter | Screened Feed | Permeate | Rejection |
|---|---|---|---|
| **Potassium ($mg \cdot L^{-1}$)** | 2626 | 2222 | 15.38% |
| **Total Nitrogen ($mg \cdot L^{-1}$)** | 4343 | 2929 | 32.56% |
| **Soluble Nitrogen ($mg \cdot L^{-1}$)** | 2929 | 2929 | 0.00% |
| **Total Phosphorus ($mg \cdot L^{-1}$)** | 1313 | 81 | 93.83% |
| **Soluble Phosphorus ($mg \cdot L^{-1}$)** | 101 | 51 | 49.50% |
| **Dry Matter (%)** | 2.7 | 0.8 | 70.37% |

The UF process using the 0.04 µm membrane showed a significant separation of suspended solids and other particulate material in the digestate. The dry matter content decreased from 2.7% in the screened feed to 0.8% in the permeate, corresponding to a membrane rejection of 70.4%, while the retentate concentration increased to 4.3%.

The membrane also had a high rejection of total phosphorus, which decreased from 1313 $mg \cdot L^{-1}$ in the feed to 81 $mg \cdot L^{-1}$ in the permeate, which corresponds to a rejection of 94%. This suggests that most of the phosphorus in the digestate was associated with particulate or colloidal material retained during filtration. In contrast, soluble phosphorus decreased from 101 $mg \cdot L^{-1}$ to 51 $mg \cdot L^{-1}$, 49.5% rejection, indicating that some of the dissolved phosphorus species were able to pass through the membrane.

Nitrogen rejection was much lower than phosphorus rejection. Total nitrogen decreased from 4343 $mg \cdot L^{-1}$ in the feed to 2929 $mg \cdot L^{-1}$ in the permeate, while soluble nitrogen remained unchanged at 2929 $mg \cdot L^{-1}$. Showing that a large fraction of nitrogen was present in dissolved form and therefore passed through the membrane. This behavior agrees with the findings of Yue et al. (2022), who reported $NH_3$-N rejection values between 20.5 and 27.3%, confirming the limited ability of UF membranes to retain dissolved nitrogen species.

Similarly, potassium showed a limited rejection, decreasing from 2626 $mg \cdot L^{-1}$ to 2222 $mg \cdot L^{-1}$ (around 15%). This result is very similar to the potassium rejection range of 1.7–15.3% reported by Yue et al. (2022). The low potassium rejection is expected since dissolved ions are generally not effectively retained by ultrafiltration membranes due to their small molecular size relative to the membrane pore size.

Barampouti et al. (2020) reported that, after digestate separation, 40–90% of phosphorus is usually concentrated in the solid fraction, whereas only 20–25% of nitrogen is retained in solids. This explains why phosphorus was more effectively removed by ultrafiltration in the present study, while dissolved nitrogen species were able to pass through the membrane more easily. Similar behaviour was also reported by Proskynitopoulou et al. (2024), who observed comparatively higher phosphorus rejection during UF treatment of digestate, while nitrogen and potassium rejection remained relatively low.

## 4.4. Nanofiltration (NF)

Figure 4.6 shows the flux for three different conditions for the nanofiltration of digestate carried out at 250 rpm, 5, 10, and 15 bar, at a temperature of 25 °C. The figure shows the pure water flux (PWF), digestate flux, pure water flux after water cleaning, pure water flux after chemical cleaning, and the corresponding flux recovery for each pressure condition.

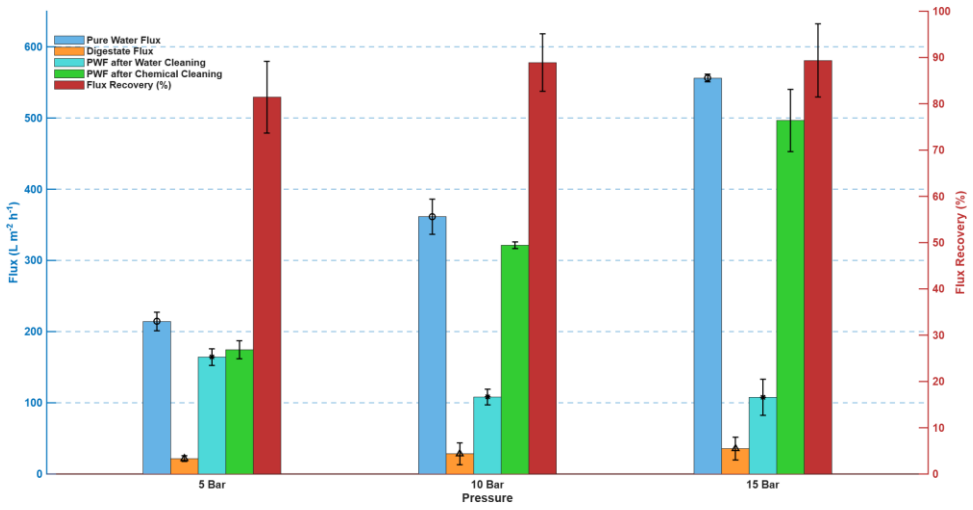


*Figure 4.6: Comparison of pure water flux (PWF), digestate flux, pure water flux after water cleaning, pure water flux after chemical cleaning, and flux recovery for three different conditions during the nanofiltration of digestate carried out at 250 rpm, 5, 10, and 15. Flux values are represented on the left y-axis, while flux recovery (%) is shown on the right y-axis.*

Similar to the ultrafiltration process, the pure water flux increased with increasing pressure, rising from 214.2 ± 12.8 $L \cdot m^{-2} \cdot h^{-1}$ at 5 bar to 361.5 ± 24.6 $L \cdot m^{-2} \cdot h^{-1}$ at 10 bar and 556.0 ± 5.3 $L \cdot m^{-2} \cdot h^{-1}$ at 15 bar. This behavior is expected, since higher operating pressure provides a greater driving force for water permeation through the membrane.

During the digestate filtration, the flux remained noticeably lower in comparison with the water flux at all pressures, with values of 21.5 ± 4.0 $L \cdot m^{-2} \cdot h^{-1}$ at 5 bar, 28.5 ± 15.6 $L \cdot m^{-2} \cdot h^{-1}$ at 10 bar, and 35.7 ± 15.8 $L \cdot m^{-2} \cdot h^{-1}$ at 15 bar.

Looking at **Figure 4.7**, which shows the change in membrane permeability with pressure, it can be seen that as the pressure increases the membrane becomes less permeable. The permeability of the membrane decreases from 4.3 $L \cdot m^{-2} \cdot h^{-1} \cdot bar^{-1}$ at 5 bar to 2.85 $L \cdot m^{-2} \cdot h^{-1} \cdot bar^{-1}$ at 10 bar and 2.38 $L \cdot m^{-2} \cdot h^{-1} \cdot bar^{-1}$ at 15 bar. This happens because higher pressure causes more particles to be forced

towards the membrane, faster deposition of solids, and a rapid formation of a cake layer, which ends up adding extra resistance, so even though the driving force increases, resistance also increases. Similar behaviour has been reported in previous membrane fouling studies by Ren et al. (2019) and Du et al. (2020), where increasing transmembrane pressure increased permeate flux but also accelerated concentration polarization and cake layer formation, resulting in greater resistance to flow and lower membrane permeability.

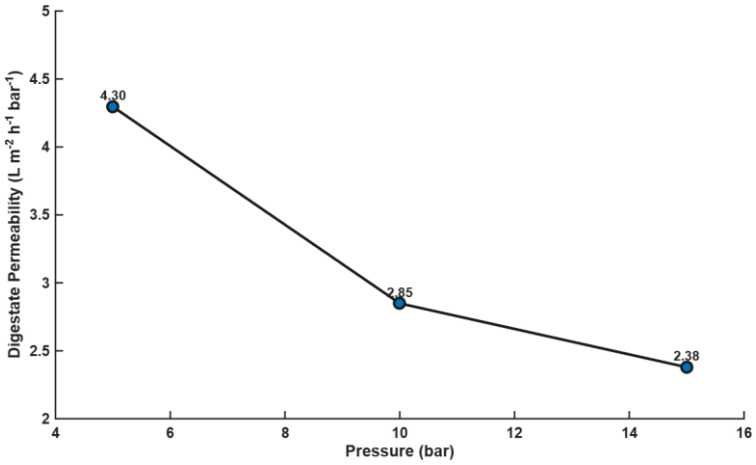


*Figure 4.7: Digestate permeability as a function of transmembrane pressure during nanofiltration.*

After digestate filtration, the pure water flux decreased compared to the initial pure water flux due to fouling formation on the membrane surface. At 5 bar, the pure water flux decreased from 214.2 ± 12.8 $L \cdot m^{-2} \cdot h^{-1}$ to 164.3 ± 11.7 $L \cdot m^{-2} \cdot h^{-1}$ after water cleaning, corresponding to a flux loss of 23.3 ± 7.3%. Similar behavior was observed at 10 and 15 bar, where the flux loss increased to 70.1% ± 3.57 and 80.6 ± 4.62%, respectively. These results are consistent with the earlier permeability trend, confirming that higher operating pressures promoted more fouling and increased resistance.

After chemical cleaning, the water flux was almost restored to approximately the initial values. At 5 bar, the recovered water flux reached 81.4 ± 8.41%. At 10 bar, the recovered flux increased to 88.9 ± 6.56%, while at 15 bar the flux recovery reached 89.3 ± 7.92%. These results indicate that most of the fouling formed during digestate filtration was removable by chemical cleaning, suggesting that a large fraction of the fouling was reversible or weakly attached to the membrane surface.

## 4.5. Reverse Osmosis (RO)

The Figure 4.8 shows the comparison of fluxes for the reverse osmosis (RO) during digestate filtration at transmembrane pressures of 15 and 18 bar. The figure presents the pure water flux (PWF), digestate flux, pure water flux after water cleaning, pure water flux after chemical cleaning, and the corresponding flux recovery values obtained at 25 °C

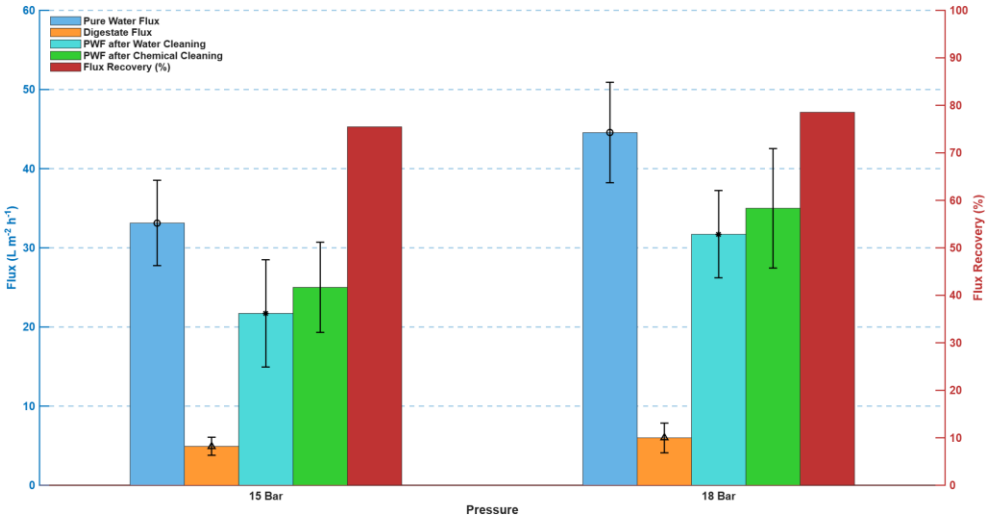


*Figure 4.8: Comparison of pure water flux, digestate flux, and recovered pure water flux after flush cleaning and chemical cleaning for the RO membrane operated at 15 and 18 bar.*

Compared to the NF membrane, the RO membrane had a significantly lower pure water and digestate fluxes due to its denser selective layer and higher resistance to flow. At 15 bar, the pure water flux was 33.1 ± 5.4 $L \cdot m^{-2} \cdot h^{-1}$, increasing to 44.6 ± 6.3 $L \cdot m^{-2} \cdot h^{-1}$ at 18 bar. Similarly, digestate flux increased slightly from 4.91 ± 1.14 $L \cdot m^{-2} \cdot h^{-1}$ to 5.99 ± 1.89 $L \cdot m^{-2} \cdot h^{-1}$ with an increase in pressure from 15 to 18 bar.

After digestate filtration, the RO membrane showed lower flux loss compared to the NF membrane, with reductions of 34.5% at 15 bar and 28.8% at 18 bar. In addition, flux recovery after chemical cleaning reached 75.4% and 78.5% at 15 and 18 bar, respectively. Unlike the NF membrane, where permeability continuously decreased with increasing pressure, the RO membrane showed a more stable behavior, suggesting that fouling development was less affected by the increase in operating pressure within the tested range.

Since the RO experiments could not be done above 18 bar due to limitations of the ALBI module (dead-end cell), the membrane behavior at higher pressures remains uncertain. Higher pressures may have resulted in more fouling and greater permeability decline.

## 4.6. Rejection after NF and RO

The Table 4.3 shows a comparison of nutrient and COD removal performance between nanofiltration (NF) and reverse osmosis (RO) membranes during digestate treatment, showing permeate concentrations and rejection efficiencies.

*Table 4.3 Feed and permeate concentrations obtained during nanofiltration (NF) and reverse osmosis (RO) treatment of digestate for nitrogen, COD, and phosphorus.*

| Parameter | Feed Concentration ($mg \cdot L^{-1}$) | NF Permeate ($mg \cdot L^{-1}$) | NF Rejection (%) | RO Permeate ($mg \cdot L^{-1}$) | RO Rejection (%) |
|---|---|---|---|---|---|
| **Nitrogen** | 2930 | 2570 | 12.3 | 1956 | 33.2 |
| **COD** | 6250 | 4470 | 28.5 | 132 | 97.9 |
| **Phosphorus** | 12.1 | 11.5 | 5.0 | 0.74 | 93.6 |

The NF membrane showed limited nitrogen rejection, with the concentration decreasing from 2930 $mg \cdot L^{-1}$ in the feed to 2570 $mg \cdot L^{-1}$ in the permeate, corresponding to a rejection of 12.3%. Similar behavior was reported by Gerardo et al. (2015), who obtained nitrogen rejection values ranging from 5 to 23.9% using the NF membranes. For phosphate, the NF membrane showed low rejection, with concentration decreasing from 12.1 $mg \cdot L^{-1}$ in the feed to 11.5 $mg \cdot L^{-1}$ in the permeate, corresponding to a rejection of approximately 5.0%. Similarly, COD concentration decreased from 6250 $mg \cdot L^{-1}$ in the feed to 4470 $mg \cdot L^{-1}$ in the permeate, corresponding to a COD rejection of 28.5%.

In contrast, the RO membrane exhibited significantly higher rejection. COD concentration decreased from 6250 $mg \cdot L^{-1}$ in the feed to 132 $mg \cdot L^{-1}$ in the permeate, corresponding to a rejection of approximately 97.9%. Similarly, phosphate concentration decreased from 12.1 $mg \cdot L^{-1}$ to 0.74 $mg \cdot L^{-1}$, resulting in a rejection of approximately 93.9%. Similar behaviour was reported by Proskynitopoulou et al. (2024), who observed phosphate rejection values of approximately 95% during RO treatment of digestate.

For nitrogen, the RO membrane reduced the concentration from 2930 $mg \cdot L^{-1}$ in the feed to 1956 $mg \cdot L^{-1}$ in the permeate, corresponding to a rejection of 33.2%. Although this rejection was higher than that obtained with the NF membrane, nitrogen removal remained lower compared to COD and phosphate removal.

Nitrogen rejection by the RO membrane remained relatively limited compared to COD and phosphate rejection. Similar behaviour has been reported in previous digestate treatment studies. (Vaneeckhaute *et al.*, 2011) reported that even after two-stage RO filtration, the permeate could still contain Nitrogen concentrations up to 820 $mg \cdot L^{-1}$, and therefore included an aerated lagoon post-treatment step to in order to reduce nitrogen concentrations in the final RO permeate.

The influence of pH on nitrogen rejection was also discussed by Camilleri-Rumbau et al. (2019), who reported that nitrogen species affect membrane rejection. At higher pH, nitrogen is more present as uncharged $NH_3$, while at lower pH it is mainly present as $NH_4^+$. Fechter and Kraume (2016) also reported that dissolved ammonia ($NH_3$) is generally not effectively retained by membranes due to its uncharged nature, it can permeate through the membrane more easily than ammonium ions ($NH_4^+$). They also explained that pH adjustment can improve nitrogen retention by converting ammonia into ammonium, which is more rejected by the membrane.

The relatively limited nitrogen rejection observed in the present study may be related to nitrogen species at the feed pH of 8.1. Although ammonium ($NH_4^+$) was likely the dominant species at this pH, part of the nitrogen would also have been present as dissolved ammonia ($NH_3$), which is uncharged and can permeate through the membrane more easily than ionic species, thereby contributing to lower nitrogen retention.

Although membrane filtration improved digestate quality, the final permeate concentration did not meet the discharge standards targeted in this study (15 $mg \cdot L^{-1}$ nitrogen, 0.1 $mg \cdot L^{-1}$ phosphorus, and 80 $mg \cdot L^{-1}$ COD). The RO membrane achieved the highest removal efficiencies, but the final permeate still had 1956 $mg \cdot L^{-1}$ nitrogen, 0.74 $mg \cdot L^{-1}$ phosphorus, and 132 $mg \cdot L^{-1}$ COD, indicating that additional post-treatment would be required, especially for nitrogen removal.

# 5. Conclusions

This study evaluated the treatment of anaerobic digestate using ultrafiltration (UF), nanofiltration (NF), and reverse osmosis (RO) membranes. Membrane performance in terms of flux, rejection, fouling, and nutrient removal efficiency were analyzed. Screening and coagulation were also investigated as pre-treatment methods to reduce solids and improve membrane filtration performance.

Screening reduced the dry matter content of the digestate by only 10%, although a large part of the solids still passed through the mesh due to the relatively large screen opening. Coagulation with $FeCl_3$ improved solids settling and phase separation in the sieved digestate, particularly at higher dosages. Due to the high solids content, it is likely that additional solids reduction prior to coagulation would have decreased the coagulant dosage.

During UF filtration, the 0.04 µm membrane maintained higher digestate flux values compared to the MF 1.2 µm membrane, likely due to increased pore blocking and cake layer formation in the larger pore membrane. UF showed high rejection of total phosphorus (93.83%), while nitrogen (32.56%) and potassium (15.38%) rejection remained limited, probably because these compounds were mainly present in dissolved form. Membrane fouling increased with increasing transmembrane pressure, resulting in reduced membrane permeability and lower flux recovery after filtration.

For NF and RO treatment, increasing pressure increased permeate flux but also accelerated fouling formation. NF showed limited rejection of nitrogen (12.3%) and phosphorus (5%), indicating low selectivity towards dissolved compounds under the tested conditions. In contrast, RO achieved significantly higher removal efficiencies, particularly for COD (97.9%) and phosphorus (93.6%). However, nitrogen rejection remained limited (33.2%), likely due to the presence of dissolved nitrogen species capable of permeating through the membrane. Among the investigated nutrients, phosphorus was removed much more effectively than nitrogen across all membrane processes

Although RO produced the best overall permeate quality, the final permeate concentration still exceeded the discharge standards targeted in this study for nitrogen, phosphorus, and COD. These results indicate that NF and single-stage RO membrane filtration alone were insufficient to fully treat the digestate to discharge quality, and that additional post-treatment steps or additional RO stages would likely be required, particularly for nitrogen removal.

# 6. Future Work

- Future studies should also evaluate using screens with smaller openings to determine if they could improve solids removal and reduce membrane fouling.
- Since nitrogen rejection remained limited during NF and RO treatment, future studies should investigate pH adjustment or additional treatment steps to improve nitrogen rejection.
- Future studies should also evaluate testing multi-stage RO to determine if systems could help achieve discharge standards for nitrogen, phosphorus, and COD.
- Further research should evaluate the effect of operating conditions such as temperature and pH on membrane fouling and nutrient rejection, particularly for nitrogen removal.
- Future membrane UF filtration experiments should investigate the effect of temperature on membrane performance and fouling behavior using systems with temperature control.
- RO filtration should also be evaluated at higher operating pressures using equipment capable of operating above 18 bar in order to better assess membrane performance under higher-pressure conditions.

# 7. Limitations

- Originally, this study was planned to use a ceramic microfiltration pilot. However, during the trials, the pilot became completely blocked due to the high solids content of the digestate and could not be used during the experimental period. As a result, a vibrating membrane system made of polymeric membranes (Vibro Lab from Sani Membranes module) was used instead.
- The ceramic membrane pilot operated under low suction pressures (- 0.03 to - 0.23 bar), resulting in a low driving force for filtration. Compared to the pressure -driven membrane filtration used later for the UF study (1 to 2 bar), this driving force may have been insufficient for the filtration of the digestate.
- Another limitation was the availability of screening equipment. Smaller sieves were not available on site during the experimental period. A 120 μm Sweco sieve, which had been used before for digestate treatment, was originally planned for this study but was not available. As a result, a larger screen was used (1mm), since it was the only one available.
- Due to limitations of the dead-end filtration cell, the operating pressure could not exceed 18 bar during the RO experiments. As a result, the behaviour of the RO membrane at higher pressures could not be evaluated.

# 8. Reference List


*About the company - Jeppo Biogas*. (2026.). Retrieved March 4, 2026, from https://jeppobiogas.fi/sv/foretaget/om-foretaget/

Ahrends, M. ;, Srivastava, H. E. ;, Sosulski, A. K. ;, Szymá Nska, M., Ahrends, H. E., Srivastava, A. K., & Sosulski, T. (2022). Anaerobic Digestate from Biogas Plants—Nuisance Waste or Valuable Product? *Applied Sciences 2022, Vol. 12, Page 4052*, *12*(8), 4052. https://doi.org/10.3390/app12084052

Alfa Laval (2024) *NF and RO spiral membranes*. Available at: https://www.alfalaval.com/globalassets/documents/products/separation/membranes/spiral-membranes/nf-and-ro-spiral/nf-and-ro-spiral-membranes-200000088-8-en-gb.pdf

Al Seadi, T., Drosg, B., Fuchs, W., Rutz, D., & Janssen, R. (2013). Biogas digestate quality and utilization. *The Biogas Handbook: Science, Production and Applications*, 267–301. https://doi.org/10.1533/9780857097415.2.267

Al Seadi, T., Drosg, B., Fuchs, W., Rutz, D., & Janssen, R. (2024). Solid-liquid separation of digestate from biogas plants: A systematic review of the techniques' performance. *Journal of Environmental Management*, *356*, 120585. https://doi.org/10.1533/9780857097415.2.267

Barampouti, E. M., Mai, S., Malamis, D., Moustakas, K., & Loizidou, M. (2020). Exploring technological alternatives of nutrient recovery from digestate as a secondary resource. *Renewable and Sustainable Energy Reviews*, *134*, 110379. https://doi.org/10.1016/J.RSER.2020.110379

Calabrò, V., & Basile, A. (2011). Fundamental membrane processes, science and engineering. *Advanced Membrane Science and Technology for Sustainable Energy and Environmental Applications*, 3–21. https://doi.org/10.1533/9780857093790.1.3

Camilleri-Rumbau, M. S., Briceño, K., Søtoft, L. F., Christensen, K. V., Roda-Serrat, M. C., Errico, M., & Norddahl, B. (2021). Treatment of Manure and Digestate Liquid Fractions Using Membranes: Opportunities and Challenges. *International Journal of Environmental Research and Public Health 2021, Vol. 18, Page 3107*, *18*(6), 3107. https://doi.org/10.3390/IJERPH18063107

Canadian Biogas Association (2024) *Digestate nutrient reuse and recovery technology summary: Supplementary materials to the Canadian Digestate Management Guide*. May 2024. Ottawa: Canadian Biogas Association.

Cathcart, A., Smyth, B. M., Lyons, G., Murray, S. T., Rooney, D., & Johnston, C. R. (2023). Optimising mechanical separation of anaerobic digestate for total solids and nutrient removal. *Journal of Environmental Management*, *345*(1), 118449. https://doi.org/10.1016/j.jenvman.2023.118449

Chuda, A., & Ziemiński, K. (2023). Ultrafiltration of digestate liquid fraction by hollow-fiber membranes: Influence of digestate pre-treatment on hydraulic capacity and nutrient removal efficiency. *Chemical Engineering Journal*, *473*, 145426. https://doi.org/10.1016/J.CEJ.2023.145426

Davis, M.L., 2010. *Water and wastewater engineering: Design principles and practice*. 1st ed. New York: McGraw-Hill Education.

Drosg, B., Fuchs, W., Al, T., Madsen, S. M., & Linke, B. (2015). *Nutrient Recovery by Biogas Digestate Processing*.

Du, X., Shi, Y., Jegatheesan, V., & Ul Haq, I. (2020). A Review on the Mechanism, Impacts and Control Methods of Membrane Fouling in MBR System. *Membranes 2020, Vol. 10, Page 24*, *10*(2), 24. https://doi.org/10.3390/MEMBRANES10020024

DuPont, 2025**.** *FilmTec™ Reverse Osmosis / Nanofiltration membranes technical manual*. Version 18, September 2025. Wilmington, DE: DuPont Water Solutions. Available at: https://www.dupont.com/content/dam/water/amer/us/en/water/public/documents/en/RO-NF-FilmTec-Manual-45-D01504-en.pdf

DuPont Water Solutions (2024) *FilmTec™ NF270 nanofiltration membrane: Product data sheet*. Available at: https://www.dupont.com/content/dam/water/amer/us/en/water/public/documents/en/NF-FilmTec-NF270-370-34-FF-PDS-45-D03432-en.pdf

European Biogas Association (2023) *Digestate and biogas: Opportunities for Europe*. Brussels: European Biogas Association.

European Biogas Association (2024) *Exploring digestate's contribution to healthy soils*. Brussels: European Biogas Association.

Fachverband Biogas e.V. (2018) *Digestate as fertilizer*. Freising: Fachverband Biogas e.V.

Fechter, M. and Kraume, M. (2016) *Digestate treatment techniques*. **Technical Transactions**, 1-M/2016, pp. 95–106.

Gent, S., Twedt, M., Gerometta, C., & Almberg, E. (2017). Introduction to Feedstocks. *Theoretical and Applied Aspects of Biomass Torrefaction*, 17–39. https://doi.org/10.1016/b978-0-12-809483-9.00002-6

Gerardo, M. L., Aljohani, N. H. M., Oatley-Radcliffe, D. L., & Lovitt, R. W. (2015). Moving towards sustainable resources: Recovery and fractionation of nutrients from dairy manure digestate using membranes. *Water Research*, *80*, 80–89. https://doi.org/10.1016/J.WATRES.2015.05.016

Hidalgo, D., Martín-Marroquín, J., Corona, F., Timmers, R. A., Sánchez-Gatón, M., & Pérez-Zapatero, E. (2026). Circular economy and biorefinery of biogas production. *Biogas: A*

*Sustainable Approach for Renewable Energy*, 1–23. https://doi.org/10.1016/B978-0-443-33679-9.00016-3

Issah, A. A., Kabera, T., & Kemausuor, F. (2020). Biogas optimisation processes and effluent quality: A review. *Biomass and Bioenergy*, *133*(10), 105449. https://doi.org/10.1016/j.biombioe.2019.105449

Jaffrin, M. Y., & Ding, L. (2015). A Review of Applications of Rotating and Vibrating Membranes Systems: Advantages and Drawbacks. *Journal of Membrane and Separation Technology*, *4*(3), 134–148. https://doi.org/10.6000/1929-6037.2015.04.03.5

Jameel, M. K., Mustafa, M. A., Ahmed, H. S., Mohammed, A. jassim, Ghazy, H., Shakir, M. N., Lawas, A. M., Mohammed, S. khudhur, Idan, A. H., Mahmoud, Z. H., Sayadi, H., & Kianfar, E. (2024). Biogas: Production, properties, applications, economic and challenges: A review. *Results in Chemistry*, *7*(7), 101549. https://doi.org/10.1016/j.rechem.2024.101549

*Jeppo Biogas hopes for greater interest in biogas - VVS Heating and Sanitary Technician*. (2026.). Retrieved March 4, 2026, from https://www.vvs-tidningen.fi/p/vvs-varme-och-sanitetsteknikern/2024-02-09/a/jeppo-biogas-hoppas-pa-ett-storre-intresse-for-biogasen/5733/1280247/47845317

Jiang, S., Zhang, Y., Zhao, F., Yu, Z., Zhou, X., & Chu, H. (2018). Impact of transmembrane pressure (TMP) on membrane fouling in microalgae harvesting with a uniform shearing vibration membrane system. *Algal Research*, *35*, 613–623. https://doi.org/10.1016/J.ALGAL.2018.10.003

Kaur, G. et al. (2020) "Value Addition of Anaerobic Digestate From Biowaste: Thinking Beyond Agriculture," Current Sustainable/Renewable Energy Reports, 7(2), pp. 48–55. Available at: https://doi.org/10.1007/s40518-020-00148-2.

Khan, O., Mufazzal, S., Khan, Z. A., Sherwani, A. F., Yahya, Z., & Alhodaib, A. (2024). Optimizing the performance parameters of vacuum evaporation technology for management of anaerobic digestate in a waste water treatment plant using fuzzy MCDM method. *Desalination and Water Treatment*, *320*(2), 100864. https://doi.org/10.1016/j.dwt.2024.100864

Mustika, P. C. B. W., Sutrisna, P. D., Sutijan, S., Petrus, H. T. B. M., Sumardi, S., & Astuti, W. (2025). Understanding membrane fouling in pressure-driven and thermal-driven processes for brines applications: challenges, mechanisms, characterization, mitigation strategies, and future perspectives. *Journal of Water Process Engineering*, *72*, 107631. https://doi.org/10.1016/J.JWPE.2025.107631

Nayak, J. K., & Ranade, V. v. (2025). Valorisation of digestate: Characteristics, products, processes and potential. *Chemical Engineering Journal Advances*, *24*. https://doi.org/10.1016/j.ceja.2025.100887

Nowak, M., & Czekała, W. (2024). Sustainable Use of Digestate from Biogas Plants: Separation of Raw Digestate and Liquid Fraction Processing. *Sustainability 2024, Vol. 16, Page 5461*, *16*(13), 5461. https://doi.org/10.3390/su16135461

Plana, P. V., & Noche, B. (2016). A Review Of The Current Digestate Distribution Models: Storage And Transport. *WIT Transactions on Ecology and the Environment*, *202*, 345–357. https://doi.org/10.2495/wm160311

Proskynitopoulou, V., Vourros, A., Garagounis, I., Dimopoulos Toursidis, P., Lorentzou, S., Zouboulis, A., & Panopoulos, K. (2024). Enhancing nutrient and water recovery from liquid digestate: A comparative study of selective electrodialysis and conventional treatment methods. *Journal of Environmental Chemical Engineering*, *12*(3), 112675. https://doi.org/10.1016/J.JECE.2024.112675

Ren, L., Yu, S., Li, J., & Li, L. (2019). Pilot study on the effects of operating parameters on membrane fouling during ultrafiltration of alkali/surfactant/polymer flooding wastewater: optimization and modeling. *RSC Advances*, *9*(20), 11111. https://doi.org/10.1039/C8RA10167A

Ren, Q., Zhang, W., Rao, P., Zhang, T., Zhang, X., Hua, Y., & Jin, S. (2026). Treatment of food waste digestate using silicon carbide membranes: Performance optimization, fouling mechanisms, and pilot-scale validation. Desalination, 626, 119994. https://doi.org/10.1016/J.DESAL.2026.119994

Selvaraj, P. S., Periasamy, K., Suganya, K., Ramadass, K., Muthusamy, S., Ramesh, P., Bush, R., Vincent, S. G. T., & Palanisami, T. (2022). Novel resources recovery from anaerobic digestates: Current trends and future perspectives. *Critical Reviews in Environmental Science and Technology*, *52*(11), 1915–1999. https://doi.org/10.1080/10643389.2020.1864957

Sherman, E. (2016) *Quantitative Characterization of Biogas Quality: A Study of Biogas Quality at Stormossen Oy*. Bachelor's thesis. Degree Programme in Energy and Environmental Engineering. Vaasa: Novia University of Applied Sciences and University of Vaasa.

Turley, D., Hopwood, L., Burns, C. and Di Maio, D., 2016. Assessment of digestate drying as an eligible heat use in the Renewable Heat Incentive. *NNFCC: York, UK*, p.28.

Ülgüdür, N. *et al.* (2019) "High-rate anaerobic treatment of digestate using fixed film reactors," *Environmental Pollution*, 252, pp. 1622–1632. Available at: https://doi.org/10.1016/J.ENVPOL.2019.06.115.

Vaneeckhaute, C., Darveau, O., & Meers, E. (2019). Fate of micronutrients and heavy metals in digestate processing using vibrating reversed osmosis as resource recovery technology. *Separation and Purification Technology*, *223*, 81–87. https://doi.org/10.1016/J.SEPPUR.2019.04.055

Vaneeckhaute, C., Meers, E., Michels, E., Christiaens, P., & Tack, F. M. G. (2011). Fate of Macronutrients in Water Treatment of Digestate Using Vibrating Reversed Osmosis. *Water,*

*Air, & Soil Pollution 2011 223:4*, *223*(4), 1593–1603. https://doi.org/10.1007/S11270-011-0967-6

Vega, E., Paredes, L., Marks, E. A. N., Singla, B., Castaño-Sánchez, O., Casas, C., Vilaplana, R., Mora, M., Ponsá, S., & Llenas, L. (2022). Application of Vibrating Reverse Osmosis Technology for Nutrient Recovery from Pig Slurry in a Circular Economy Model. *Membranes*, *12*(9), 848. https://doi.org/10.3390/MEMBRANES12090848/S1

Waeger, F., Delhaye, T., & Fuchs, W. (2010). The use of ceramic microfiltration and ultrafiltration membranes for particle removal from anaerobic digester effluents. *Separation and Purification Technology*, *73*(2), 271–278. https://doi.org/10.1016/J.SEPPUR.2010.04.013

Xavier, L.D., Yokoyama, L., de Oliveira, V.R., Ribeiro, G.T. & Araújo, O., 2020. The role of coagulation-flocculation in the pretreatment of reverse osmosis in power plant. Journal of Sustainable Development of Energy, Water and Environment Systems, 8(1), pp.118–131. https://doi.org/10.13044/j.sdewes.d7.0272

Yue, C., Chen, Y., Zhang, W., Zheng, Y., Hu, X., & Shang, B. (2022). Direct Purification of Digestate Using Polymeric Ultrafiltration Membranes: Influence of Materials on Filtration Behavior and Fouling Characteristics. *Membranes 2022, Vol. 12, Page 882*, *12*(9), 882. https://doi.org/10.3390/MEMBRANES12090882

Zhao, Y., Zhang, Y., Xing, B., Xu, W., & Yin, Z. (2025). Developments in vibrating membrane filtration systems. *Journal of Industrial and Engineering Chemistry*, *148*, 131–149. https://doi.org/10.1016/J.JIEC.2025.01.017

Zhao, Z., Muylaert, K., & F.J. Vankelecom, I. (2023). Applying membrane technology in microalgae industry: A comprehensive review. *Renewable and Sustainable Energy Reviews*, *172*, 113041. https://doi.org/10.1016/J.RSER.2022.113041

Zhu, X., Chi, X., Duan, Y., Li, C., Yun, M., Ma, J., Zhang, Z., Shen, B., Kong, W., & Wang, Z. (2026). Review on multifaceted recycling of anaerobic digestate: Nutrient utilization and thermochemical conversion. *Journal of Environmental Chemical Engineering*, *14*(1), 120821. https://doi.org/10.1016/J.JECE.2025.120821

Zielińska, M. and Mikucka, W. (2021) "Membrane filtration for valorization of digestate from the anaerobitreatment of distillery stillage," *Desalination and Water Treatment*, 215, pp. 60–68. Available at: https://doi.org/10.5004/DWT.2021.26772.

# 9. Appendices

*Table 9.1: Average permeate flux () and standard deviation (SD) for pure water flux (PWF), digestate ultrafiltration flux, and pure water flux after chemical cleaning using the **1.2 µm ultrafiltration membrane** at transmembrane pressures of 1 and 2 bar. Flux recovery (%) after chemical cleaning is also presented.*

| **Pressure** | **1 Bar** | | **2 Bar** | |
|---|---|---|---|---|
| **Parameter** | **Average Flux ($Lm^{-2}h^{-1}$)** | **SD** | **Average Flux ($Lm^{-2}h^{-1}$)** | **SD** |
| **Pure Water Flux (PWF)** | 335.6 | 20.184 | 379.886 | 40.507 |
| **Digestate Flux** | 1.294 | 0.449 | 4.333 | 2.099 |
| **PWF after Chemical Cleaning** | 72.531 | 5.129 | 152.629 | 22.999 |
| **Flux Recovery (%)** | 21.6 | 1.9 | 40 | 7 |

*Table 9.2: Composition of screened feed, retentate, and permeate streams after ultrafiltration using a 0.04 µm membrane.*

| **Parameter** | **Screened Feed** | **Retentate** | **Permeate** |
|---|---|---|---|
| **Potassium (mg/L)** | 2626 | 2525 | 2222 |
| **Total Nitrogen (mg/L)** | 4343 | 4949 | 2929 |
| **Soluble Nitrogen (mg/L)** | 2929 | 3131 | 2929 |
| **Total Phosphorus (mg/L)** | 1313 | 1919 | 81 |
| **Soluble Phosphorus (mg/L)** | 101 | 111 | 51 |
| **Dry Matter (%)** | 2.7 | 4.3 | 0.8 |

*Table 9.3: Average permeate flux (J) over time during ultrafiltration of digestate using the **1.2 µm ultrafiltration membrane** at 1 and 2 bar presented in 5-minute intervals with corresponding standard deviations (SD).*

| Interval (min) | Average Flux ($Lm^{-2}h^{-1}$) at 1 Bar | SD | Average Flux ($Lm^{-2}h^{-1}$) at 2 Bar | SD |
|---|---|---|---|---|
| **0–5** | 1.808 | 0.128 | 8.914 | 1.524 |
| **5–10** | 1.87 | 0.198 | 6.343 | 0.618 |
| **10–15** | 1.582 | 0.128 | 5.2 | 0.262 |
| **15–20** | 1.418 | 0.163 | 4.8 | 0.514 |
| **20–25** | 1.623 | 0.094 | 3.771 | 0 |
| **25–30** | 1.151 | 0.304 | 3.6 | 0 |
| **30–35** | 0.949 | 0.155 | 3.171 | 0.121 |
| **35–40** | 0.814 | 0.071 | 2.914 | 0.242 |
| **40–45** | 0.781 | 0.036 | 2.743 | 0.242 |
| **45–50** | 0.822 | 0.036 | 2.4 | 0.242 |
| **50–55** | 0.814 | 0.161 | 2.314 | 0.121 |
| **55–60** | 0.781 | 0.031 | 2.143 | 0.121 |

*Table 9.4: Average permeate flux (J) and standard deviation (SD) for pure water flux (PWF), digestate ultrafiltration flux, and pure water flux after chemical cleaning using the **0.04 µm ultrafiltration membrane** at transmembrane pressures of 1 and 2 bar. Flux recovery (%) after chemical cleaning is also presented.*

| **Pressure (Bar)** | **1** | | **1.5** | | **2** | |
|---|---|---|---|---|---|---|
| **Parameter** | **Average Flux ($Lm^{-2}h^{-1}$)** | **SD** | **Average Flux ($Lm^{-2}h^{-1}$)** | **SD** | **Average Flux ($Lm^{-2}h^{-1}$)** | **SD** |
| **Pure Water Flux (PWF)** | 54.909 | 2.666 | 104.336 | 11.318 | 226.857 | 16.199 |
| **Digestate Flux** | 3.795 | 1.377 | 4.696 | 1.004 | 6.833 | 2.432 |
| **PWF after Chemical Cleaning** | 40.200 | 1.707 | 58.063 | 5.718 | 110.971 | 12.105 |
| **Flux Recovery (%)** | 73.213 | 4.75 | 55.650 | 8.19 | 48.917 | 6.40 |

*Table 9.5:Average permeate flux (J) over time during ultrafiltration of digestate using the 0.04 µm membrane at a transmembrane pressure of 1, 1.5 and 2 bar, presented in 5-minute intervals with corresponding standard deviations (SD).*

| **Pressure** | **1 Bar** | | **1.5 Bar** | | **2 Bar** | |
|---|---|---|---|---|---|---|
| **Interval (min)** | **Average Flux ($Lm^{-2}h^{-1}$)** | **SD** | **Average Flux ($Lm^{-2}h^{-1}$)** | **SD** | **Average Flux ($Lm^{-2}h^{-1}$)** | **SD** |
| **0–5** | 6.927 | 0.443 | 6.574 | 0.407 | 13.296 | 1.574 |
| **5–10** | 5.166 | 0.538 | 5.048 | 0.203 | 10.83 | 1.004 |
| **10–15** | 4.344 | 0.269 | 4.755 | 0.176 | 8.189 | 0.626 |
| **15–20** | 3.757 | 0.566 | 4.755 | 0.305 | 7.308 | 0.102 |
| **20–25** | 3.287 | 0.102 | 3.874 | 0.352 | 6.956 | 0.61 |
| **25–30** | 3.346 | 0.176 | 3.64 | 0.102 | 6.222 | 0.102 |
| **30–35** | 3.236 | 0.514 | 3.757 | 0.102 | 5.811 | 0 |
| **35–40** | 2.73 | 0.125 | 3.581 | 0.102 | 5.635 | 0.249 |
| **40–45** | 2.642 | 0.135 | 3.61 | 0.203 | 5.107 | 0.499 |
| **45–50** | 2.818 | 0.167 | 3.17 | 0.176 | 4.843 | 0.102 |
| **50–55** | 2.836 | 0.249 | 3.17 | 0.102 | 4.491 | 0.125 |
| **55–60** | 2.201 | 0.125 | 3.082 | 0.102 | 4.461 | 0.444 |

*Table 9.6: Pure water flux (PWF), digestate flux, PWF after water and chemical cleaning, flux loss, and flux recovery percentages during nanofiltration of digestate at operating pressures of 5, 10, and 15 bar. Flux values are expressed as average permeate flux with corresponding standard deviations (SD).*

| **Pressure** | **5 Bar** | | **10 Bar** | | **15 Bar** | |
|---|---|---|---|---|---|---|
| **Parameter** | **Average Flux ($Lm^{-2}h^{-1}$)** | **SD** | **Average Flux ($Lm^{-2}h^{-1}$)** | **SD** | **Average Flux ($Lm^{-2}h^{-1}$)** | **SD** |
| **Pure Water Flux (PWF)** | 214.247 | 12.793 | 361.487 | 24.610 | 555.950 | 5.33646 |
| **Digestate Flux** | 21.48 | 3.974 | 28.4875 | 15.557 | 35.691 | 15.8373 |
| **PWF after Water Cleaning** | 164.319 | 11.677 | 108.118 | 10.984 | 107.760 | 25.5024 |
| **PWF after Chemical Cleaning** | 174.480 | 12.9 | 321.321 | 4.788 | 496.652 | 43.6616 |
| **Lost Flux (%)** | 23.30 | 7.26 | 70.09 | 3.57 | 80.62 | 4.62 |
| **Flux Recovery (%)** | 81.44 | 8.41 | 88.89 | 6.56 | 89.33 | 7.92 |

*Table 9.7: Average permeate flux expressed in and corresponding standard deviations (SD) measured during nanofiltration of digestate at operating pressures of 5, 10, and 15 bar over a 60-minute filtration period.*

| **Pressure** | **5 Bar** | | **10 Bar** | | **15 Bar** | |
|---|---|---|---|---|---|---|
| **Interval (min)** | **Average Flux ($Lm^{-2}h^{-1}$)** | **SD** | **Average Flux ($Lm^{-2}h^{-1}$)** | **SD** | **Average Flux ($Lm^{-2}h^{-1}$)** | **SD** |
| **0–5** | 27.83 | 1.15 | 56.33 | 4.16 | 59.65 | 18.92 |
| **5–10** | 27.17 | 2.29 | 51.03 | 2.29 | 56.34 | 3.98 |
| **10–15** | 21.87 | 1.99 | 47.06 | 1.99 | 51.03 | 6.05 |
| **15–20** | 23.86 | 2.29 | 40.43 | 3.03 | 46.4 | 4.97 |
| **20–25** | 20.55 | 3.56 | 25.17 | 2.29 | 45.07 | 9.83 |
| **25–30** | 19.88 | 5.3 | 20.55 | 2.99 | 32.48 | 7.63 |
| **30–35** | 19.22 | 4.79 | 14.58 | 4.16 | 34.47 | 8.14 |
| **35–40** | 18.6 | 4.16 | 18.5 | 1.8 | 29.83 | 7.95 |
| **40–45** | 18.56 | 1.15 | 17.8 | 1.6 | 24.52 | 9.4 |
| **45–50** | 17.8 | 1.15 | 17.2 | 1.4 | 17.9 | 7.17 |
| **50–55** | 16.51 | 0.9 | 16.8 | 1.2 | 16.2 | 2.1 |
| **55–60** | 15.91 | 0.8 | 16.4 | 1 | 14.4 | 1.8 |

*Table 9.8: Pure water flux (PWF), digestate flux, PWF after water and chemical cleaning, flux loss, and flux recovery percentages during reverse osmosis filtration of digestate at operating pressures of 15 and 18 bar. Flux values are expressed as average permeate flux with corresponding standard deviations (SD).*

| **Pressure** | **15 Bar** | | **18 Bar** | |
|---|---|---|---|---|
| **Parameter** | **Average Flux ($Lm^{-2}h^{-1}$)** | **SD** | **Average Flux ($Lm^{-2}h^{-1}$)** | **SD** |
| **Pure Water Flux (PWF)** | 33.124 | 5.397 | 44.556 | 6.345 |
| **Digestate Flux** | 4.908 | 1.144 | 5.990 | 1.889 |
| **PWF after Water Cleaning** | 21.710 | 6.801 | 31.712 | 5.515 |
| **PWF after Chemical Cleaning** | 24.998 | 5.695 | 34.996 | 7.548 |
| **Lost Flux (%)** | 34.46 | 22.82 | 28.83 | 16.25 |
| **Flux Recovery (%)** | 75.44 | 20.54 | 78.54 | 20.28 |